MASTERARBEIT / MASTER'S THESIS

Titel der Masterarbeit / Title of the Master's Thesis

"Analysis of CRaf - Rok-α Interaction"

verfasst von / submitted by

Bertram Aschenbrenner BSc

angestrebter akademischer Grad / in partial fulfilment of the requirements for the degree of

Master of Science (MSc)

Wien 2016 / Vienna 2016

Acknowledgements

Kurzfassung

Der Raf/Mek/ERK Signalweg ist der am meisten studierte aus der Mitogen aktivierten Protein Kinasen Familie. In den 30 Jahren intensiver Untersuchungen der Ras zu ERK Signaltransduktion wurden auch unabhängige Interaktionen und Funktionen neben ERK Aktivierung, von den involvierten Kinasen, gefunden und weiter studiert. Im speziellen CRaf ist bekannt mit anderen Proteinen außerhalb des ERK Signalweges zu interagieren. Demnach, neben Ras, BRaf und Mek ist Rok-α ein Bindungspartner von CRaf. Rok-α ist Teil des Rho Signalweges und verbindet Rho mit LIM Kinase. Die Aktivierung von CRaf führt nicht nur zu CRaf – BRaf Dimerisierung, sondern ebenfalls zu CRaf – Rok-α Dimer Formierung. Für BRaf Dimerisierung ist eine intakte CRaf Kinase Domäne essentiell, wohingegen für Dimerisierung mit Rok-α die N-Schleife von CRaf ausreichend ist. Allerdings wird die Interaktion beim Vorhandensein der Kinase Domäne von CRaf verstärkt. Trotz der Tatsache, dass für beide, BRaf und Rok-α, die Interaktion mit CRaf die CRaf Kinase Domäne involviert ist, konkurriert BRaf und Rok-α nicht um die Bindung an CRaf. Der Phosphorylierungszustand von CRaf S621 unterscheidet Rok-α Bindung von BRaf Bindung. Möglicherweise führt der Phosphorylierungszustand von CRaf S621 zu einer Veränderung der Konformation der Kinase Domäne welche diese molekulare Unterscheidung von Bindungspartnern ermöglicht.

Abstract

The Raf/Mek/ERK pathway is the most studied among the mitogen activated protein kinase family. In 30 years of intense investigations of Ras to ERK signaling, independent interactions and functions besides kinase dependent ERK activation were identified and further investigated. Especially CRaf is known to interact with proteins beyond the ERK signaling pathway.

Rok-α is binding partner of CRaf and part of the Rho-pathway that links Rho to LIM kinase. Activation of CRaf does not only lead to CRaf-BRaf dimerization, but also to CRaf-Rok-α dimer formation. For BRaf dimerization an intact CRaf kinase domain is essential while for Rok-α dimerization instead the N-lobe of CRaf is sufficient. However, the interaction between Rok-α and CRaf is further increased in the presence of the kinase domain of CRaf. In spite the fact that both BRaf and Rok-α interactions with CRaf involve the CRaf-kinase-domain, BRaf and Rok-α do not compete for CRaf binding. The phosphorylation state of CRaf at S621 discriminates between Rok-α binding and BRaf binding, possibly directing the kinase domain of CRaf to a different conformation, thereby mediating a conformation-dependent BRaf or Rok-α specificity.

Inhaltsverzeichnis

Abbreviations

MAPK	Mitogen activated protein kinase
CRaf	C - Rapidly Accelerated Fibrosarcoma
Rok-α	Rho-associated protein kinase
Grb2	Growth factor receptor bound protein 2
GEF	Guanine nucleotide exchange factor
SOS	Son of sevenless
Ras	Rat sarcoma
GDI	Guanine Dissociation Inhibitor
GPCR	G protein coupled Receptor
RBD	Ras binding domain
LIMK1	LIM domain kinase 1
ECL	Enhanced chemiluminescence
IP	Immunoprecipitation
LB	Luria broth
PBS	Phosphate buffered saline
FCS	Fetal calf serum
CRD	Cysteine rich domain
DMEM	Dulbecco's Modified Eagle Medium
DMSO	Dimethyl sulfoxide
PBS	Phosphate-buffered saline
BSA	bovine serum albumin
PVDF	Polyvinylidene fluoride
DAPI	4',6-diamidino-2-phenylindole

1   Introduction

1.1   Mitogen activated protein kinases

The mitogen-activated protein kinases (MAPK) ERK1/2, JNK, p38 and ERK5 become activated following the binding of growth-factors, hormones and cytokines to their respective receptors. ERK1/2, the best characterized pathway, was shown to regulate important cellular mechanisms such as proliferation, differentiation, survival, senescence and migration. The pathway consists of Ras, the downstream target Raf, MEK and ERK. MAP3K (Raf) activates the MAP2K, MEK, which in turn activates the MAPK, ERK (**Figure 1**). This pathway provides a central molecular link between the membrane and the nucleus (Mebratu & Tesfaigzi 2009).
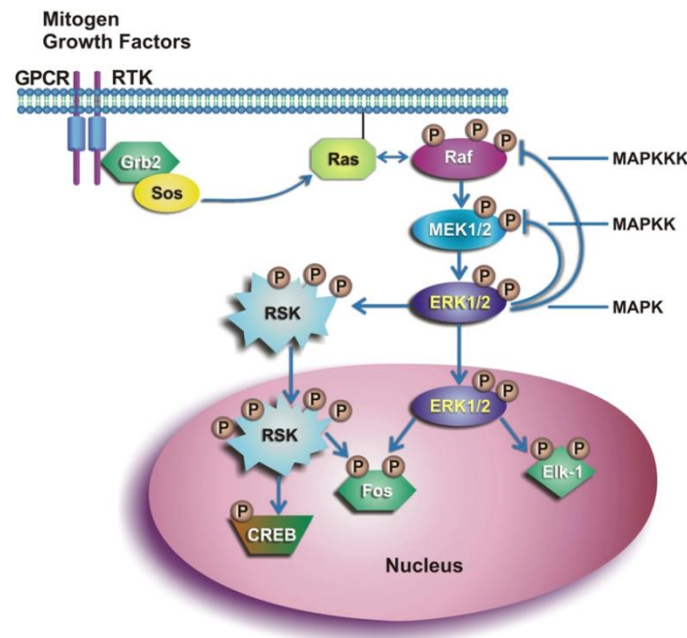
Figure 1 Mechanism of ERK activation and cell proliferation *(Mebratu & Tesfaigzi 2009)*. Signaling from the extracellular space through the cytoplasm into the nucleus by the MAPK pathway.

Activation of the pathway is initiated upon ligand binding to the extracellular receptor of a receptor tyrosine kinase or a G protein-coupled receptor. This event leads to an intracellular response and the recruitment of the adaptor Grb2 (growth factor receptor bound protein 2) and the GEF (guanine nucleotide exchange factor) SOS (son of sevenless). SOS activates Ras, a small GTPase. In the human genome three genes encode Ras; HRas, NRas, KRas. Ras cycles between the inactive GDP bound and

active GTP bound state. Cycling is regulated by guanine nucleotide exchange factors (GEFs), GTPase activating proteins (GAPs) and Guanine Dissociation Inhibitors (GDIs). GDIs inhibit the release of GDP, and as a consequence, inactivate Ras (Newlaczyl et al. 2014). GTP-loaded Ras initiates the recruitment of Raf to the plasma membrane. Subsequently, Raf dimerization takes place and induces Raf catalytic activity. Raf activates MEK, which activates ERK1/2. ERK1/2 is translocated to the nucleus where it interacts with transcription factors and influences transcription of survival and growth related genes. ERK1/2 can also phosphorylate cytosolic proteins. Depending on the site of phosphorylation, such interaction can activate or inhibit ERK partners. ERK also feeds back on the upstream-kinases and SOS to down-regulate signaling after stimulation (Mebratu & Tesfaigzi 2009)

1.2 Raf in malignancies

RAF was discovered more than 30 years ago. Soon, evidence arose that Raf is connected to malignant neoplasia. In 2002 Davies et al. (Davies et al. 2002) showed that BRAF is altered in many different tumors (e.g.: metastatic melanoma, papillary thyroid carcinoma with a frequency over 50%). In general the ERK1/2 pathway is activated in ~30% of human tumors (Santarpia et al. 2012).

Cancer is a universal term for a large group of diseases that can affect any part of the body. Cancer cells need to acquire a number of essential properties to build up malignant neoplasms: sustained proliferative signaling, evasion of growth suppression, replicative immortality, resistance to cell death, induction of angiogenesis and ability to invade tissue and form metastasis. Other abilities, such as evasion from the immune system, induction of inflammation, metabolic deregulation, and genome instability together with the accumulation of mutations over time collectively support tumor growth (Hanahan & Weinberg 2011).

The ability to invade the surrounding tissue and even spread throughout the body, called metastasization, is the major cause of death from cancer (http://www.who.int/cancer/en/).

BRAF and CRAF are also subject to germline mutations associated with RASopathies; Noonan syndrome, LEOPARD syndrome and cardio-facio-cutaneous syndrome (Niihori et al. 2006; Rodriguez-Viciana et al. 2006; Pandit et al. 2007; Razzaque et al. 2007; Rauen 2013).

1.3   Structure and regulation of CRAF

CRaf consists of 3 conserved regions: The N-terminal Ras-binding domain (RBD) and the Cysteine-rich domain (CRD), the C-terminal kinase domain and a regulatory region in-between these domains. The full-length crystal structure of CRaf is not yet available, but the partial crystal-structures describing three regions have been solved: The RBD, the CRD and the kinase domain with its N-lobe and C-lobe. The RBD is located at the N-terminus between residue 56 and 131 (Emerson et al. 1995). The next known structure is the CRD close to the RBD from residue 136 to 187 (Mott et al. 1996). Furthermore, the kinase domain close to the C-terminus that consists of a small N-lobe (residue 340 to 426) and a big C-lobe has been characterized (residue 426 to 648) (Hatzivassiliou et al. 2010) (**Figure 2**).
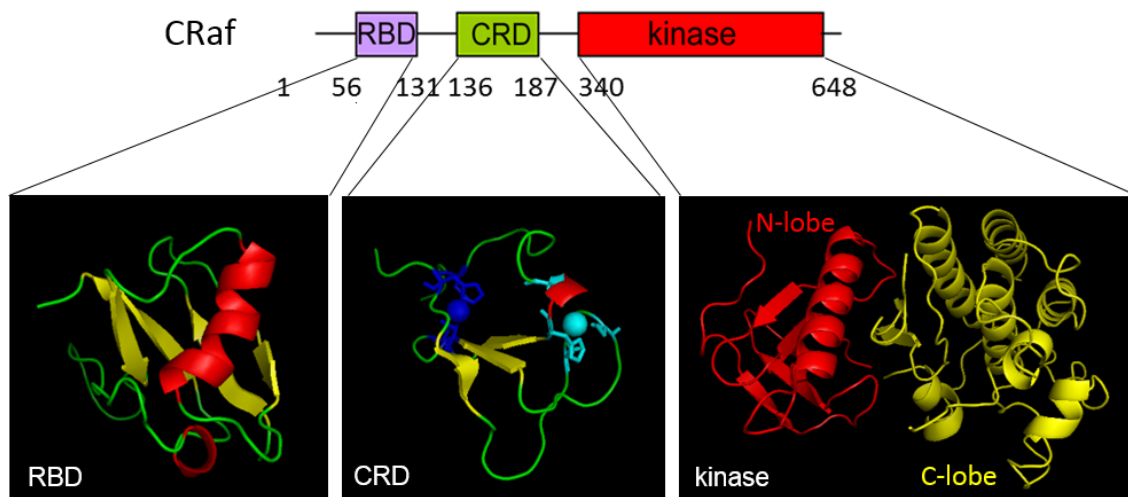
Figure 2 Cartoon of CRaf's domains and their published structures *(Emerson et al. 1995; Mott et al. 1996; Hatzivassiliou et al. 2010)*

CRaf is regulated at multiple levels. After translation, protein quality control takes place. Only when S621 is autophosphorylated by CRaf in cis, degradation by the proteasome is prevented. The folding process is mediated by HSP90 and HSP70. If S621 is not phosphorylated, the E3 ubiquitin ligase CHIP (C terminus of Hsp70-interacting protein) ubiquitinates CRaf leading to its degradation (**Figure 3**). After S621 phosphorylation, the adaptor protein 14-3-3 can bind to CRaf and stabilizes its tertiary structure (Noble et al. 2008).
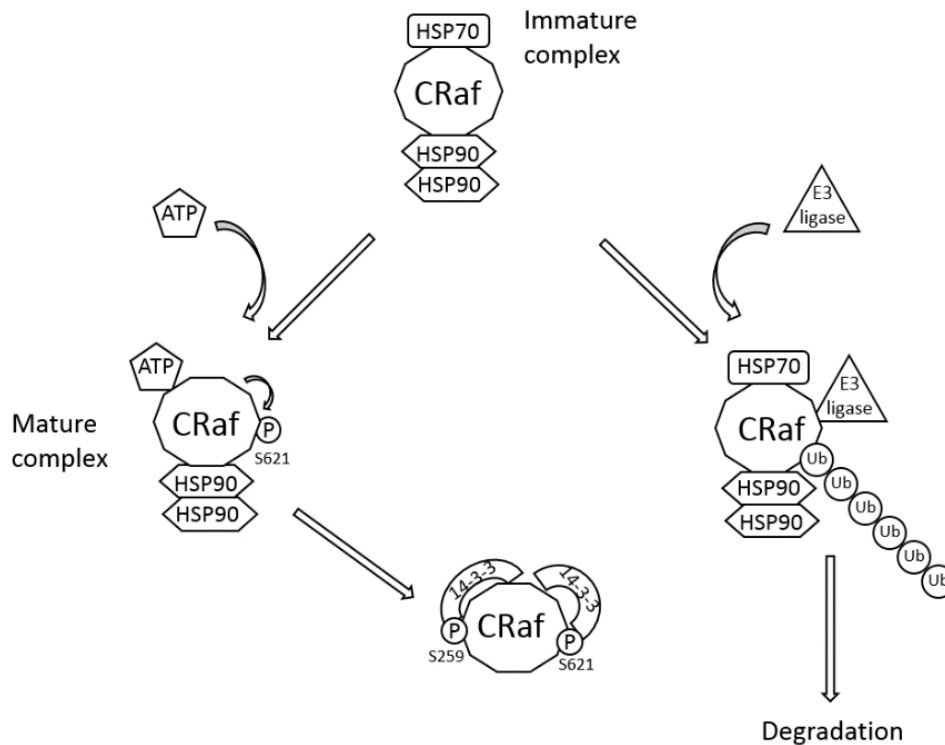
Figure 3 S621 auto-phosphorylation prevents CRaf degradation by the proteasome (adapted from *(Noble et al. 2008)*)

Regulation of CRaf by phosphorylation-dephosphorylation events and by 14-3-3 proteins

The adaptor protein 14-3-3 (mainly its ε and ζ isoforms) was identified as an interaction partner of CRaf (Fischer et al. 2009) by mass spectrometry. CRaf contains three regions, which might bind to 14-3-3 proteins. One of them is S621 that is localized at the C-terminus. This site was shown to have a role in binding to BRaf and thus in the stabilization of the RAF heterodimer, and also in MEK/ERK phosphorylation. Another site, S259, is localized in the N-terminal regulatory region of CRaf. The dephosphorylation of this site has a role in Ras binding, thus in the activation of CRaf (reviewed in Lavoie & Therrien 2015 (Lavoie & Therrien 2015)). Other groups also identified a further 14-3-3-binding site, located at S233, and showed that binding of 14-3-3 ζ to pS233 and pS259 inhibits the recruitment of CRaf to the membrane as also the dimerization of CRaf with BRaf (Molzan & Ottmann 2012). In resting cells S259, S233 and S621 are phosphorylated (Dhillon et al. 2007). Upon activation of Ras and recruitment of CRaf to the membrane, phosphatases are activated to remove the phosphorylations on S233 and S259. This change in charge allows Ras to bind to the RBD of CRaf and to induce a conformational change allowing dimerization. Following dimerization, T491 and S494 that are located in the activation loop become phosphorylated (Chong et al. 2001). Activation loop phosphorylation is induced by dimerization with another RAF molecule working as an activator, and occurs in cis by autophosphorylation (Hu et al.

2013). Subsequently, activating phosphorylations of S338 by CaMKII (Salzano et al. 2012) or MEK (Hu et al. 2013) and Y341 by Src take place (Salzano et al. 2012). When ERK is activated it will phosphorylate CRaf on six negative regulatory phospho-sites (serines and threonines), leading to a desensitized state of CRaf. In this state, all phosphorylations are removed from CRaf by phosphatases which allow kinases (PKA, PKB) to reestablish the S233 and S259 phosphorylation and 14-3-3 can bind again (Molzan & Ottmann 2012).
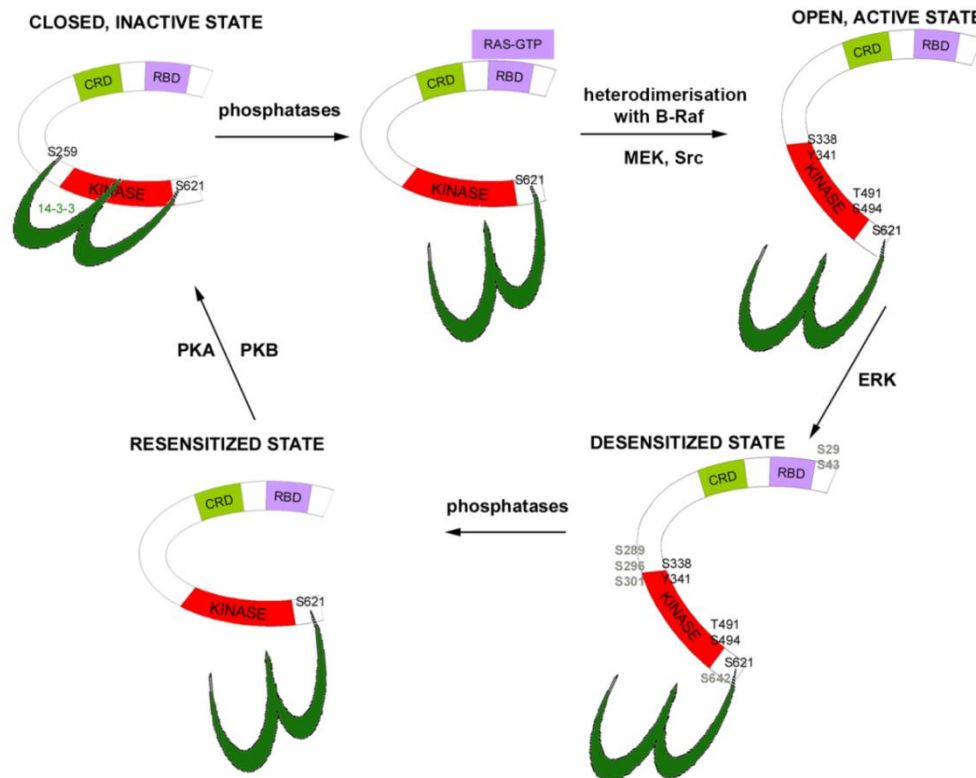
Figure 4 Regulation of CRaf by phosphorylation and 14-3-3 binding (Varga & Baccarini 2012)

1.4 Rho/Rok-α pathway

The Rho GTPase family consists of 3 subfamilies, Rho (A/B/C), Rac (1/2/3) and CDC42 (cell divisions cycle-42(CDC42Hs and G25K))(Miyazaki et al. 2006). The Rho-pathway is involved in cytoskeleton organization and dynamics (actin and microtubule), gene transcription, oncogenic transformation and cell cycle progression. Rho GTPases (like Ras GTPases) cycle between GTP and GDP bound states. Cycling is regulated by guanine nucleotide exchange factors (GEFs), GTPase activating proteins (GAPs) and Guanine Dissociation Inhibitors (GDIs). GDIs inhibit the release of GDP, which

leads to inactivation of Rho. Rho is activated mainly through GPCRs which induce the GTP bound state. Activated RhoA interacts with and activates a variety of targets, including Rok-α (Nakamura et al. 2006). Rok-α mediates downstream signaling by inducing Thr508 phosphorylation in the activation loop of LIMK1 (Ohashi et al. 2000). LIMK1 further interacts with Cofilin (Bravo-Cordero et al. 2013). Cofilin promotes the depolymerization of actin filaments, unless phosphorylated on Ser3 by LIMK1 (Riento & Ridley 2003). Phospho-Cofilin has other functions in the cell, e.g. it inhibits STAT3 which acts as a transcription factor for Myc. Myc regulates the expression of a variety of genes involved in cell growth, and is frequently altered in cancer (Dominguez-Sola et al. 2007).

1.5   Regulation and structure of Rok-α

Rok-α consists of an N-terminal kinase domain followed by a long coiled-coil-region. The RBD (Rho binding domain) is localized close to the C-terminal end of the coiled-coil domain. Rok-α further contains a cysteine-rich PH-domain (plekstrin homology domain) that is located at the C-terminus of Rok-α (**Figure 5**)(Julian & Olson 2014).

Figure 5 Cartoon of the Rok-α domains *(Julian & Olson 2014)*. ROCK2 is a synonym for Rok-α

A similar mechanism of regulation has been hypothesized for Rok-α and CRaf, although Rok-α regulation is less well studied. In both cases, the inactive state of the kinases is characterized by a closed conformation where the kinase-domains interact with the regulatory cysteine-rich domains. These interactions have to be released to turn these proteins into competent kinases. Ras binding to CRAF or Rho binding to Rok-α promotes the translocation of these proteins to subcellular sites where they can be further activated by upstream kinases/phosphatases, initiating the conformational change that makes the kinase-domain accessible for its substrates. In addition, Rho independent activation of Rok-α, through cleavage of the autoinhibitory domain by Caspase 3 or Granzyme B, has been reported (**Figure 6**).
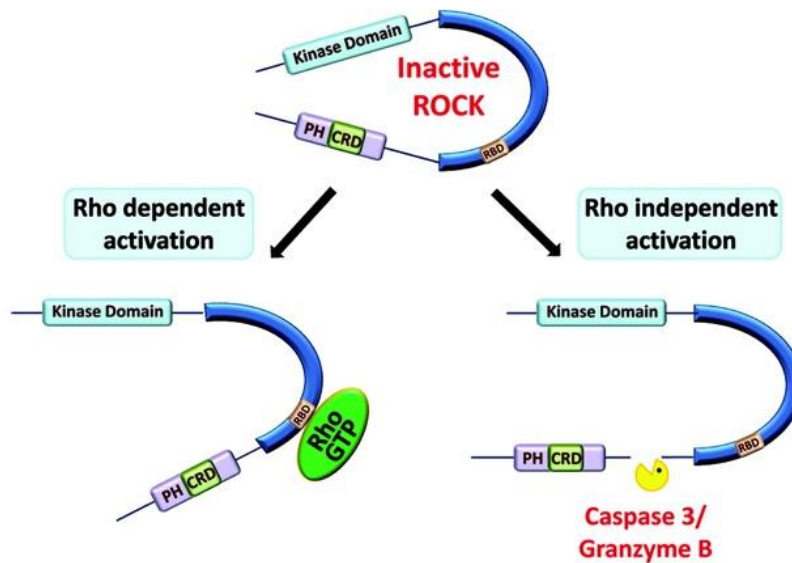
Figure 6 Rok-α activation, the Rho dependent and Rho independent way of Rok-α activation *(Julian & Olson 2014).*

1.6   CRaf–Rok-α interaction

As mentioned above (1.5), CRaf and Rok-α are similarly regulated. In inactive state, the kinase domain of both proteins is bound intramolecularly to the regulatory domain. By stimulation of Ras or Rho, autoinhibition is relieved. Negative regulation of kinases through other kinases is well known to be mediated by phosphorylation. For example, ERK phosphorylates activated CRaf on several inhibitory sites to induce deactivation (Varga & Baccarini 2012). Inhibition of Rok-α by CRaf is mediated by protein-protein interaction in a kinase independent manner. Rok-α interacts more extensively with the open state of CRaf. This was shown by reducing Rok-α to its kinase domain or removing its PH/CRD. Stimulation of mouse embryonic fibroblasts by EGF also increased CRaf Rok-α interaction. Previous experiments showed that CRaf does not bind to the Rok-α autoinhibitory domain but rather to the Rok-α kinase domain (Niault et al. 2009).

It was suggested that the CRaf regulatory domain represents the main binding region of Rok-α. Co-transfection of Rok-α kinase domain with CRaf regulatory domain showed similar results to co-transfection of Rok-α kinase domain with Rok-α regulatory domain. Both regulatory domains are able to reduce the increase in pEzrin, which appears by overexpressing Rok-α kinase domain in Cos-1 cells (Niault et al. 2009).

CRaf regulatory domain and Rok-α co-localize on vimentin filaments, which collapse upon phosphorylation by Rok-α. In CRaf knockout MEFs vimentin collapses, but transfection with the CRaf regulatory domain rescues this phenotype by down regulating hyperactive Rok-α (Niault et al. 2009).

The biological relevance of the CRaf-Rok-α interaction has been shown in several ways: Rok-α is required for the maintenance of cell shape and migration of fibroblasts. Depletion of CRaf leads to deregulation and incorrect localization of Rok-α. That results in defects in shape and migration (Ehrenreiter et al. 2005). Angiogenic sprouting requires CRaf for recruiting Rok-α to adherent junctions, where Rok-α mediates MLC2 phosphorylation (Wimmer et al. 2012). Importantly, CRaf has a critical role in initiating and maintaining squamous cell carcinoma development by inhibiting Rok-α-induced keratinocyte differentiation (Ehrenreiter et al. 2009). CRaf mediated Rok-α inhibition leads to a decrease in expression of epidermal differentiation cluster genes. The epidermal differentiation complex (EDC) comprises a large number of genes that are of crucial importance for the maturation of the human epidermis (Marenholz et al. 2001). In addition, the decrease in cofilin phosphorylation affects the phosphorylation and activation of STAT3, a transcription factor, which induces Myc expression (Varga & Baccarini 2012).
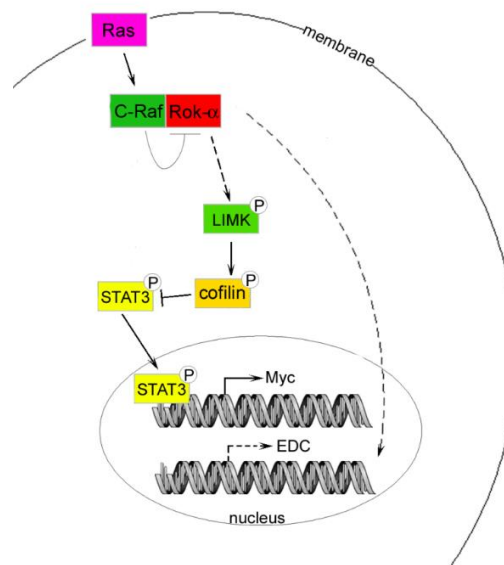
Figure 7 Pathway crosstalk of CRaf with Rok-α (Varga & Baccarini 2012)

1.7 Aim of the study

The primary aim of my master study was to gain insight into the molecular mechanism of CRaf - Rok-α interaction. A plethora of information has been gathered on this interaction prior to the start of my master thesis project. However, several open questions remained.

In the course of this study I concentrated on characterizing the interaction of CRaf with Rok-α in order to reveal which domains of these two molecules physically interact. Furthermore, I focused my attention on the characterization of the intracellular localization of this complex. Finally, I aimed for a detailed description of 14-3-3 adaptor protein-dependent regulation of CRaf binding to BRaf and Rok-α.

2   Materials and Methods

2.1   Bacterial cell culture

2.1.1   Competent cells

Top10 cells were inoculated in 20 ml LB medium. After letting them grow overnight at 37°C, 200 µl of the culture were transferred in 20 ml LB. The culture should reach a density with an absorbance of 0.5 to 0.6 at 600 nm at 37°C on the shaker. The cells were cooled down on ice for 15 minutes and centrifuged for 15 minutes at 4000 rpm and 4°C. The pellet was resuspended in 5 ml cold-sterile Tfb-I buffer and centrifuged again for 15 minutes with 4000 rpm and 4°C.

2 ml of Tfb-II buffer were gently added and centrifugation was carried out for 15 minutes at 4000 rpm and 4°C. The competent bacteria were aliquoted (100 µl per tube) and frozen in liquid nitrogen and stored at -80°C.

Tfb-I:
30 mM KOAc; 50 mM $MnCl_2$; 100 mM KCl; 10 mM $CaCl_2$; 15 % (w/v) Glycerol.

Tfb-II:
10 mM Na-MOPS pH 7.0; 75 mM $CaCl_2$; 10 mM KCl; 15 % (w/v) Glycerol.

Heat-shock transformation

1 µl of DNA (plasmid) was used to transform 100 µl of Top10 cells (Top10 cells were prepared and stored at -80°C until used). The DNA was added to the cells, followed by incubation for 20 minutes on ice, continued by a heat-shock for 80 seconds at 42°C. Afterwards, the bacteria were cooled down on ice for one minute. Then 350 µl Luria broth-medium were added. The bacteria were incubated at 37°C for one hour.

- For mini-prep, bacteria were inoculated in 5-20 ml LB (1:1000→100 µg/ml (100 mg/ml stock) antibiotics [ampicillin]) and grown overnight at 37°C on the shaker.

- For maxi-prep, bacteria were inoculated in 4 ml media and after approximately 6 hours 500 µl were transferred in 200-250 ml LB-media conatinaing antibiotics and grown overnight at 37°C on the shaker.

- Alternatively transformed bacteria were plated on LB-agar plates. On the next day (after approximately 16 hours) single colonies were picked and inoculated in 10 ml LB-media. The inoculated colony was placed on a shaker at 37°C overnight. On the next day a Miniprep-Kit was used to isolate the transformed plasmid.

Luria broth-media: 8 g NaCl

8 g Tryptone

4 g Yeast Extract

add 800 ml to dH_2O

The media was autoclaved before usage.

Luria broth-agar plates: 5 g NaCl

5 g Tryptone

2.5 g Yeast Extract

7.5 g Agar

add dH_2O to 500 mL

After autoclave-sterilization 500 µl Ampicillin were added and the media was poured into plates.

2.1.2   Isolation of plasmids from E. *coli*

The Mini-Kit was used to lyse and purify DNA. 20 ml LB-Medium with antibiotics (ampicillin) were used for each picked *E. coli* colony that contained the plasmid with insert of interest. Single colonies were expanded overnight.

2.1.2.1   Protocol

The bacteria were centrifuged for 10 minutes at 3900 rpm. The pellet was resuspended in 250 µl resuspension-buffer and transferred into an Eppendorf-tube. 250 µl lysis-solution were added and after approximately 1 minute, 350 µl neutralization-solution were used to neutralize the lysis. The lysed bacterial pellet was transferred onto a filter-membrane-tube and centrifuged 1 minute at 13 krpm. The membrane was washed two times with wash-solution (500 µl centrifuge 1 minute at 13 krpm). Ethanol was removed by centrifugation, 1 minute at 13 krpm. The membrane was incubated with elution-solution for 4 minutes and the eluate containing the DNA was centrifuged into a fresh tube.

Nucleic acid concentration was measured by using the Nano-drop spectrophotometer.

Restriction digest: To test, whether antibiotic resistant bacteria carried the insert of interest, a restriction digest was performed.

2.1.3   Maxi prep

Preparation for the Maxi prep (day before)**:** Competent Top 10 *E. coli* were used to amplify plasmids. 1 µl DNA (concentration between 500-1500 ng/µl) was added to 100

µl Top10 cells. After 20 minutes incubation on ice, *E. coli* were heat-shocked for 80 seconds at 42 C°. After cooling on ice for 1 minute, 350 µl LB-medium were added and the bacteria were kept at 37 °C for 1 hour. The bacteria were transferred into 4 ml LB-media with 4 µl ampicillin (100 µg/ml) and kept on 37°C until they reached the desired cell density (between 5-7 hours, dependent on the efficiency of the ligation). 500 µl were transferred into 200 ml LB-media with 100 µg/ml ampicillin and grown overnight.

On the next day the preparation was started by pelleting the bacteria at 10000 g for 5 minutes. Plasmid isolation was performed according to the PerfectPrep™ EndoFree Maxi Kit manuals (GmbH 2009).

2.1.4   Agarose-gel

1% Agarose-gels were used to separate DNA (50 ml TAE-buffer with 0, 5 g Agarose plus 1 µg/ml ethidium-bromide). 10 µl probe were mixed with 2 µl 6x-loading-dye and loaded onto the slots of the gel. As Ladder the Thermo Scientific GeneRuler 1kb DNA Ladder was used. The DNA was separated by 88 V for 35 minutes.

Finding a positive hit on the gel needed to be confirmed by sequencing: a sample having a volume between 10 and 20 µl with a concentration between 100 and 200 ng/µl was sent to VBC-BIOTECH Service GmbH and later on to LGC Genomics.

2.1.5   PCR

The different CRaf truncations and mutants were generated by PCR. The primers were designed and ordered and PCR was performed with CRaf full length DNA as a template. The program of the thermo-cycler was adjusted to the melting temperature of the primers and the optimal working temperature of the polymerase was used to amplify the DNA of interest. The right annealing temperature and duration of each cycle had to be adapted. After amplifying the DNA, the template was digested using the enzyme Dpn1.

CRaf truncations, Rok-kinase and Rok-full-length were produced by PCR with designed primers. CRaf was tagged with FLAG, Rok-kinase-domain with HA.

2.2   Cell culture

Dulbecco's Modified Eagle Medium (DMEM): 4500 mg/l glucose and L-glutamine

Complete medium: Penicillin and Streptomycin 1:1000, 10% FCS (50 ml) and 500 ml DMEM.

Starvation medium: Penicillin and Streptomycin 1:1000 in 500 ml DMEM.

Freezing medium: 90% FCS and 10% Dimethyl sulfoxide (DMSO)

10x PBS: NaCl [AppliChem Panreac]   1.37 M

KCl [AppliChem Panreac]   26.8 mM

Na_2HPO_4 [AppliChem Panreac]   101.43 mM

KH_2PO_4 [AppliChem Panreac]   21.6 mM

Set to pH 7.4

2.2.1   Transfection

Starvation medium was added to the cells after washing twice with 1xPBS (20 minutes before transfection). DNA was mixed with starvation medium in an Eppendorf tube, then PEI (Polyethylenimine) was added (1:2 ratio). The mixture was incubated for 20 minutes at room temperature. This mixture was put drop-wise onto the cells. The dish was mixed and placed back at 37 °C for 3 to 4 hours. The medium was exchanged to complete medium. Cells were harvested the next day.

2.2.2   Cell splitting

Adherent cells have to be split once they reach a confluent state. The growing of most fibroblasts is limited by contact inhibition. Fibroblasts change their behavior at a specific point and should be split before that happens.

The medium was removed and the plates were washed twice with 1xPBS. Trypsin was added to the plates to remove the anchors of the cells (2 ml per 15 cm dishes/1 ml per 10 cm dishes, the cells were incubated for 2-3 minutes at 37 °C). Differences between attached and detached cells can be seen in the microscope. At the right moment 5-times volume of medium over trypsin was added to inhibit the reaction. The cells were resuspended from the plate and the cell number was counted with the microscope. The desired number of cells was plated.

2.2.3   Starvation

The cells were starved by using 0% FCS DMEM-medium containing antibiotics. Starvation was done to synchronize the culture. The old media was removed, washed once with 1xPBS, PBS was removed and starvation medium was added (8-10 ml/15 cm dish, 4 ml/10 cm dishes, 1 ml/6 well plate).

2.3   Protein analysis

2.3.1   Materials

Lysis buffer for COS 7 cells (Tris-Triton buffer):

   200 mM Tris [AppliChemPanreac]

   2 mM EDTA [AppliChem Panreac]

   1% Triton X-100 [Sigma Aldrich]

   pH 7.4

Add inhibitors just before use:

   1 mM PMSF

   0.1 mM Na_3VO_4 (sodium orthovanadate)

   10 nM ocadaic acid

   1 Protease inhibitor cocktail tablet, complete, EDTA-free with different Inhibitors inside [Boehringer Mannheim] for 50 ml lysis buffer

PMSF stock 0.1 M (dissolve 17 mg Phenylmethylsulfonylfluorid in 1 ml isopropanol) [Fluka]

Ocadaic acid 100 mM (25 µg ocadaic acid use 311 µl of DMSO) [Calbiochem]

10x PBS		
	NaCl [AppliChem Panreac]	1.37 M
	KCl [AppliChem Panreac]	26.8 mM
	Na_2HPO_4 [AppliChem Panreac]	101.43 mM
	KH_2PO_4 [AppliChem Panreac]	21.6 mM
	Set to pH 7.4	

BSA (bovine serum albumin) standard Pierce BCA (bicinchroninic acid) Protein Assay [Thermo Scientific]

Sample buffer (Laemmli):

0.32M Tris [AppliChem Panreac],

5% SDS [AppliChem Panreac],

50% Glycerol [AppliChem Panreac],

0.008% Bromphenolblue [Merck/BDH],

pH 6.8

5x sample buffer (SB): 1 ml SB plus 143 µl 2-Mercaptoethanol [Sigma]

SDS-PAGE: Separating buffer: 1.5 M Tris, pH 8.8

Stacking buffer: 0.5 M Tris, pH 6.8

2.3.2   Lysis of cells

The plates were placed on ice, the medium was sucked off and the plates were washed 3-times with cold 1xPBS. Lysis-buffer was added (500 µl per 10 cm dishes, 800 µl per 15 cm dishes and 145 µl per 6-well plate). The cells were scraped from the plates and transferred into a 1.5 ml pre-cooled centrifuge tube. The lysates were vortexed for 5 seconds and placed on a rotation wheel for 20 minutes continued for 20 minutes centrifugation at 20000 g. The supernatant was transferred into a new tube.

2.3.3   Protein concentration measurement

Proteins were incubated with BCA (Pierce bicinchronic acid) (50 µl dH$_2$O plus 3 µl protein plus 200 µl BCA) for 30 minutes in a 96 well plate. The absorbance was measured at 570 nm. To calculate the sample concentration, the absorbance of a dilution-series of BSA standard was measured at the same time. The linear range of the concentration was calculated from a standard curve. To maximize the accuracy, all samples were measured two times and the protein-concentration was calculated from the average absorbance.

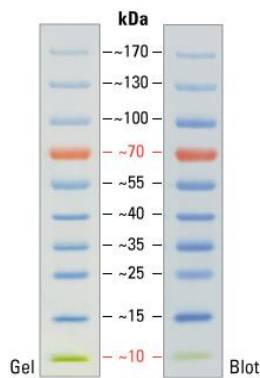### 2.3.4   SDS-PAGE

Small gels: in the stacking gel constant 60 V were used; for separation of proteins constant 120 V were used.

Wide gels: 0,03 A/gel in the stacking gel, and 0,06 A/gel for the separating gel.

4 % stacking gel was used continued by a 7, 5 % or 12 % separating gel.

The protein marker used was from thermoscientific (PageRuler Prestained Protein Ladder (see **Figure 8**)):

Figure 8 SDS-PAGE band profile of the PageRuler Prestained Protein Ladder
(Prestained & Ladder 2009)

2.3.5   Western-Transfer

Wide gels: The gel was incubated for 15 minutes in transfer buffer; this improved the efficiency of the transfer. Assembly: Sponge-2x whatman paper-PVDF-gel-2x whatman paper-Sponge.

The transfer was done over 16 hours with 200 mA, continued by 2 h 400 mA. Small transfer: The transfer was assembled the same way. It was run at 250 mA for 1h. PVDF (Polyvinylidene fluoride) membrane bound the proteins. The proteins were labeled with specific antibodies for immuno-detection.

2.3.6   Immuno-detection

Proteins from the gel were boud to the PVDF membrane. To detect the proteins of interest, specific antibodies were used. The membrane was put into blocking solution for 30 minutes. The unbound milk was washed away with TBST two times for 5 minutes. The membrane was incubated overnight with the primary antibody. On the next day, the membranes were washed again 3 times 5 minutes. The secondary antibody was added for 45 minutes. Afterwards, un-bound secondary antibody was washed away through incubating three times for 10 minutes in TBST. Secondary antibodies were coupled with HRP (horseradish peroxidase). HRP catalyzes a reaction that yields chemiluminescence using specific substrates. ECL pico and ECL prime were used (enhanced chemiluminescence kit) to visualize antibody-labeled proteins. High sensitivity films were used to visualize the membrane bound proteins in the dark.

2.3.7   Stripping membranes

Several different antibodies can be used for labeling the same PVDF membrane, since these can be removed from PVDF membranes by stripping.

15 minutes cooking of the PVDF membranes in ddH$_2$O removed antibodies that had bound to protein. After removing the antibodies, the membrane was treated as described before starting after the point of western-transfer.

To store membranes, the salt of TBST had to be removed to prevent crystallization. One washing step with water was done. Membranes were kept at -20 °C after drying.

2.3.8   Used Tags

HA human influenza hemagglutinin. The sequence is: YPYDVPDYA

FLAG-tag: FLAG is an octapeptide with the sequence: DYKDDDDK

The sequence was added by recombinant DNA technology to the protein of interest. The tags were used for immunoprecipitation, and for antibody-dependent detection of proteins on membranes.

2.3.9   Immunoprecipitation

Antibody-Antigen complexes were used to separate proteins from cell lysates. I mainly used immunoprecipitation (IP) to enrich FLAG-tagged CRaf constructs, which were transfected in COS7 cells and used for studying the co-immunoprecipitation of the co-transfected Rok-α kinase. In theory, only proteins that interact with the immunoprecipitated protein are found in the purified fraction.

40 µl of a 50 % FLAG-Beads solution per IP was prepared: The beads were delivered in a glycerol solution and had to be washed: wash 3 times with ~1 ml cold PBS from Sigma (spin at 500g for 2 min), add the same volume PBS → 50% washed FLAG beads.

40 µl washed FLAG-beads were added to each tube (clean tubes and filter tips were used to avoid contamination). 150 µg lysate was added to each tube, filled up with appropriate lysis buffer to 500 µl and incubated for 1 hour at 4 °C on the rotating wheel. The procedure was continued by washing 6x with cold Lysis buffer (aspirate the supernatant, add 1 ml cold Lysis buffer, turn 15x upside down, spin 2 minutes; 500 g; 4°C). 30 µl of 2x Sample buffer were added (320 µl 5x + 480 µl LB), cooked for 3 minutes at 95 °C, transferred to a new Eppendorf tube (the pipet was set to a higher volume than expected, the immunoprecipitation was transferred to new tubes with thin loading tips). The volume was adjusted with 1x Sample buffer for each sample.

Following, the IP was loaded onto the gels.

The second type of IP was done with CRaf/Rok-α/BRaf antibodies which were bound to G-Sepharose beads. 150 µg cell lysate were incubated overnight at 4 °C on a rotating wheel with 4 µg of the respective antibody (20 µl of 200 µg/ml). On the next day,

40 µl of 50 % G-Sepharose beads were put in an Eppendorf-tube and the cell lysate with the antibodies were added to the beads. After 2 hours incubation at 4 °C on a rotating wheel each sample was washed five times with lysis buffer. 30 µl 2x Sample buffer (320 µl 5x Sample buffer + 480 µl Lysis buffer) was added, cook for 3 minutes at 95 °C, transferred to a new Eppendorf-tube (the pipet was set to a higher volume than expected, the immunoprecipitation was transferred to new tubes with thin loading tips). The volume was adjusted with 1x Sample buffer.

Materials:

Anti-FLAG® M2 affinity gel

Raf-1 C20 200 µg/ml

Rok-α C20 200 µg/ml

BRaf H-145 200 µg/ml

2.3.10 Immunofluorescence

Anti-HA and anti-FLAG primary antibodies were used to target the HA-tagged Rok-α kinase domain, and FLAG-tagged CRaf wild type and CRaf S233A/S259A mutant. Secondary antibodies used: Alexa Fluor® 488 for FLAG antibody and Alexa Fluor® 546 for HA antibody.

800000 Cos7 cells were seeded on 10 cm dishes with coverslips inside the dish. On the next day the cells were transfected with three different setups: Empty vector, HA-Rok-α kinase domain together with FLAG-CRaf wild type, HA-Rok-α kinase domain together with FLAG-CRaf S233A/S259A mutant.

On the next day the coverslips with the attached cells were washed twice with cold 1x phosphate buffered saline, fixed with 4 % paraformaldehyde for 10 minutes and washed 2 minutes with cold 1x PBS. The cells were permeabilized with 0.2 % Triton in 1x PBS for 5 minutes at room temperature, washed 2 minutes with cold 1x PBS. Next quenching was performed using 0.1 M Glycine in 1x PBS for 10 minutes at room temperature, washed 2 minutes with cold 1x PBS and blocked with 3 % fetal calf serum in 1x PBS for 30 minutes at 37 °C. Primary antibodies were diluted in 1 % FCS in 1x PBS and were incubated for 1.5 hours at room temperature. Excessive primary antibody was washed-off 3 times for 5 minutes with 1x PBS followed by incubation with the secondary antibody and phalloidin diluted in 1 % FCS in 1x PBS for 45 minutes at room temperature in the dark. After washing 3 times for 5 minutes with 1x PBS, nuclear staining was performed with 4′, 6-Diamidin-2-phenylindol in 1x PBS 1:3000 for 5

minutes. Samples were again washed 3 times for 2 minutes with 1x PBS and washed once with water prior to drying. The dried coverslips were mounted with ProLong® Gold Antifade Mountant on microscopy slides and dried at room temperature overnight in the dark. Mounted coverslips were fixed to the slide with nail polisher on the next day.

Materials:

Primary antibodies:

HA rabbit polyclonal (Cell Signaling 1:3200)

FLAG goat polyclonal (BETHYL DDDDK 1:600)

Phalloidin Alexa Fluor® (680 nm) 1:200

Secondary antibodies:

Alexa Fluor® donkey anti-rabbit (546 nm) 1:1,500

Alexa Fluor® donkey anti-goat (488 nm) 1:1,500

2.3.11 Proximity ligation assay

PLA is a method that is used to demonstrate the close proximity of two proteins of interest. Primary antibodies produced in two different species are used to target the proteins. The secondary antibodies are coupled with a unique short DNA strand (minus and plus). With a ligase, the short DNAs are ligated if they are close to each other (max. distance between the secondary antibodies is 16 nm, which is slightly more than for resonance energy transfer between fluorophores with 10 nm (Trifilieff et al. 2013)). By rolling circle replication the ligated DNA is amplified. The used oligonucleotides are labeled by a fluorophore which gives a visible dot for every interaction.

Duolink® In Situ Detection Reagents Green:

Blocking solution

Antibody diluent

Wash buffer A: 0.01 M Tris, 0.15 M NaCl 0.05% Tween 20, pH 7.4

Wash buffer B: 0.2 M Tris, 0.1 M NaCl pH 7.5

1x Ligase (1 unit/µl)

5x Amplification Green: Contains oligonucleotides labeled with a fluorophore and all other components needed for Rolling Circle Amplification.

1x Polymerase (10 units/µl)

Raf-1 Abcam ab154754 rabbit polyclonal 1:1000

RockII Santa Cruz sc-1851 goat polyclonal 1:2000

Phalloidin Alexa Fluor® (680 nm) 1:200

800000 Cos7 cells were seeded on 10 cm dishes with coverslips inside the dish. On the next day the cells were transfected. On the following day the cover slips with the attached cells were washed twice with cold 1x PBS and fixed with 4% paraformaldehyde for 10 minutes. They were washed for 2 minutes with cold 1x PBS, permeabilized with 0.2 % Triton in 1x PBS for 5 minutes at room temperature. After that, the coverslips were washed again for 2 minutes with cold 1x PBS. Quenching was done in 0.1 M Glycine in 1x PBS for 10 minutes at room temperature (this step decreases the autofluorescence intensity of formaldehyde and therefor the background signal). Samples were washed again for 2 minutes with cold 1x PBS. Blocking was carried out with blocking solution for 30 minutes at 37 °C. Incubation with primary antibodies in antibody diluent was performed at 4 °C overnight. Next morning, the coverslips were washed twice quickly and three times 10 minutes with Wash buffer A. They were washed once quickly with 1x PBS, fixed again with 4 % paraformaldehyde for 10 minutes, washed once quickly with 1x PBS and 3 times 10 minutes with Wash buffer A. The two PLA Probes were diluted 1:5 in Antibody diluent and incubated for 20 minutes. The PLA Probe solution was added on the coverslips and incubated for 1 hour at 37 °C. The non-bound secondary antibodies were washed 2 times quickly and 3 times for 10 minutes with Wash buffer A, then washed once quickly with 1x PBS and fixed again with 4% PFA for 10 minutes. Excess PFA was washed away once quickly with 1x PBS, then quenching was carried out with 0.1M Glycine in 1x PBS for 10 minutes at room temperature. Quenching solution was washed away once quickly with 1xPBS and 3 times for 10 minutes with Wash buffer A. The ligation stock was diluted 1:5 in high purity water and mixed. The ligase was added to the ligation solution 1:40, and the Ligation solution containing the Ligase was placed on each sample and incubated for 30 minutes at 37 °C. The coverslips were washed with Wash buffer A 4 times for a total of 5 minutes. Duolink Amplification stock was diluted 1:5 in high purity water and mixed. The Amplification-Polymerase was added to the amplification solution (1:80) and put on the samples for 100 minutes at 37 °C. The samples were washed twice with 1 x Wash Buffer B for 5 minutes. 1x Wash Buffer B with DAPI 1:3000 was put on the samples for 2 minutes, which were further washed once with 0.01x Wash Buffer B for 1 minute. The coverslips were dried and mounted with ProLong® Gold Antifade Mountant on microscopy slides. They were dried overnight at room temperature in dark. The mounted coverslips were fixed to the slide with nail polisher.

Immunofluorescence pictures and proximity ligation assay experiments were analyzed and recorded with a LSM710 confocal microscope.

3　Results

3.1　CRaf truncations

By investigating the structure of CRaf, the question arises which domains are involved in its binding to BRaf and Rok-α. To determine which domain or domains of CRaf are important for the interaction with Rok-α, different truncated forms of CRaf were tested. The constructs were chosen based on domain boundaries or on the basis of the presence of a negative regulatory phosphorylation sites (S233, S259) of CRaf (**Figure 2**, **Figure 4**).

3.1.1　N-terminal truncations

CRaf N-terminal truncations were produced and transfected in Cos7 cells (**Figure 9**). Rok-α kinase showed similar expression levels in all lysates; the 303-648 and the 258-648 FLAG-CRaf constructs were expressed best compared to the other 3 constructs. Nevertheless, the amounts of immunoprecipitated FLAG-CRaf constructs were mostly equal. Only the 426-648 and the 258-648 CRaf constructs were slightly less immuno-precipitated. This may be due to folding problems of some constructs that form soluble aggregates in which the FLAG-tag is hidden so that the specific antibody cannot bind. As shown by western blot, Rok-α kinase domain binds to all five CRaf constructs. Even the 426-648 construct, which contains just the C-lobe of the kinase domain, was able to bind Rok-α.
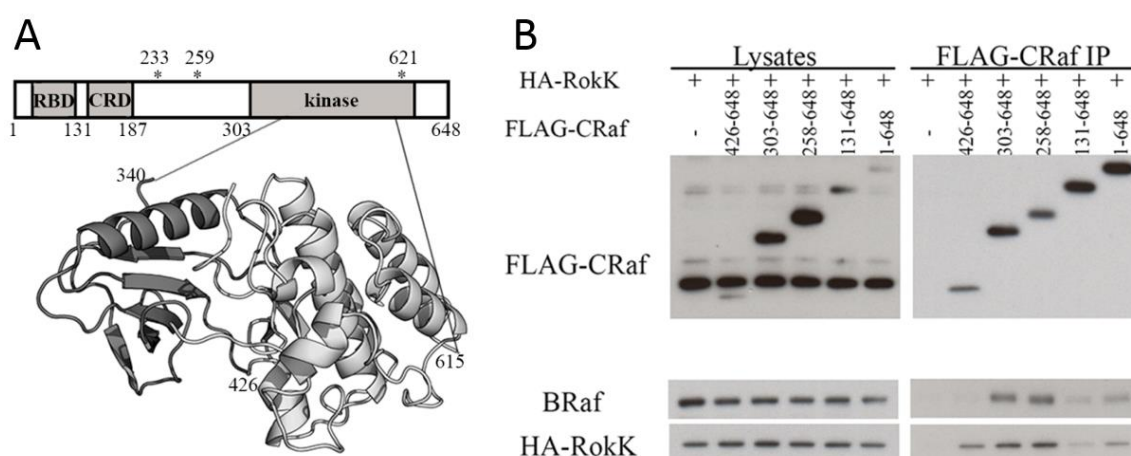
Figure 9 A: **Schematic representation of CRaf protein together with the known structure of its kinase domain B: Immunoprecipitation experiment with N-terminal truncations**

Cos7 cells were co-transfected with HA-tagged Rok-α kinase domain (1-543) and the indicated FLAG-tagged CRaf constructs which differ in length. CRaf was immunoprecipitated from the cells using FLAG-antibody. The co-precipitated HA-Rok kinase and endogenous BRaf are visualized by HA and BRaf antibodies.

3.1.2 C-terminal truncations

Prior to starting my Master thesis, I tested the effect of C-terminal truncations of CRaf on Rok-α binding in Cos7 cells (**Figure A1**). The 1-426 construct (containing the N-terminal part of CRaf and the small lobe of its kinase domain, (see **Figure 2** for the CRaf structure) and the 1-648 full length construct showed similar binding strength (**Figure A1**). These results suggested that the large lobe of the kinase domain of CRaf is not necessary to bind to Rok-α. The 1-303 construct (N-terminal regulatory domain of CRaf only, without the kinase domain) exhibited a strong reduction in binding efficiency compared to the wild type and the 1-426 CRaf. All shorter constructs except construct 1-226 behaved similar to construct 1-303. The binding efficiency of construct 1-226 was better than the other truncated versions of CRaf. Possibly because this construct does not contain the two regulatory phosphorylation sites (S233, S259) that may negatively affect CRaf-Rok-α binding. By truncating CRaf to its RBD, binding to Rok-α was further decreased.

Since the binding of construct 1-426 compared to 1-648 did not show any difference in the C-truncation experiment (**Figure A1**), we can conclude that the C-lobe is not necessary for binding, but the C-lobe construct 426-648 does bind to Rok-α by itself. Rok-α also interacted better with constructs containing the CRaf kinase domain and lacking the N-terminal regulatory domains (258-648 and 303-648) than with full-length CRaf; in contrast, removal of the CRaf Ras-binding-domain (131-648) led to decreased CRaf-Rok-α interaction compared to the full length protein (**Figure 9**).

In addition, I investigated the binding of the endogenous BRaf to CRaf in Cos7 cells. The interaction of the full-length CRaf and BRaf was visible (**Figure A1**). All C-terminal truncations of CRaf failed to bind BRaf. These experiments show that an intact CRaf kinase domain is necessary for the interaction with BRaf.

3.1.3 Additional N-terminal truncation-study

The previous experiment demonstrated that the 1-426 construct is fully competent to bind Rok-α. To find the smallest possible construct which still possesses a similar binding strength to Rok-α, I truncated the 1-426 construct from its N-terminus. The results revealed that the residues preceding the RBD domain (1-56) are not necessary for binding, while instead both the RBD and CRD are necessary (**Figure A2**).

BRaf requires an intact kinase domain on CRaf to allow interaction (**Figure A1**). These results could be confirmed by the N-terminal truncation experiment. The 426-648 construct did not interact with BRaf (**Figure 9**). By adding the N-lobe of the kinase (303-648), BRaf-CRaf interaction was detectable. This was also true for construct 258-648. By adding the autoinhibitory cysteine rich domain (131-648) the interaction decreased. These result are consistent with a role of the autoinhibitory cysteine rich domain in the induction of a closed, inactive conformation of CRaf (Varga & Baccarini 2012) (**Figure 4**). The presence of the Ras binding domain has also a regulatory effect on CRaf-BRaf dimer formation. CRaf lacking the Ras binding domain is not activatable by Ras, therefore it remains in the closed inactive state, and less frequently, heterodimerizes with BRaf. The comparison of the full-length (1-648) to the 131-648 construct revealed that the full-length construct co-immunoprecipitated more BRaf (**Figure 9**).

3.2 CRaf regulation by 14-3-3

After analyzing which domains of CRaf are important for dimerization with Rok-α and BRaf, I also wanted to study the impact of 14-3-3-binding phosphorylation sites on the CRaf Rok-α interaction. In addition, I wanted to investigate whether (and if yes, how) CRaf discriminates between BRaf and Rok-α.

The regulation of CRaf in terms of activation of the ERK1/2 pathway has been investigated in great detail (reviewed in Lavoie & Therrien 2015). Several regulatory phosphorylation sites have been shown to be relevant for activation and inactivation of CRaf (Lavoie & Therrien 2015). I decided to focus on the 14-3-3 binding sites of CRaf that are regulated by kinases and phosphatases.

14-3-3 binding to CRaf was not significantly affected by the S233A single mutant (**Figure 10**). On the other hand, a S259A mutant dramatically decreases CRaf – 14-3-3 binding, which was further reduced in a CRaf S259AS233A mutant. The faint remaining signal possibly represents C-terminal binding of 14-3-3 protein to residue S621. The S621A mutant showed a very moderate decrease in 14-3-3 co-immunoprecipitation. Finally, the double and triple mutants (S621AS259A and S621AS259AS233A) did not show any detectable 14-3-3 interaction. Thus, pS259 is the main 14-3-3 binding site on CRaf.
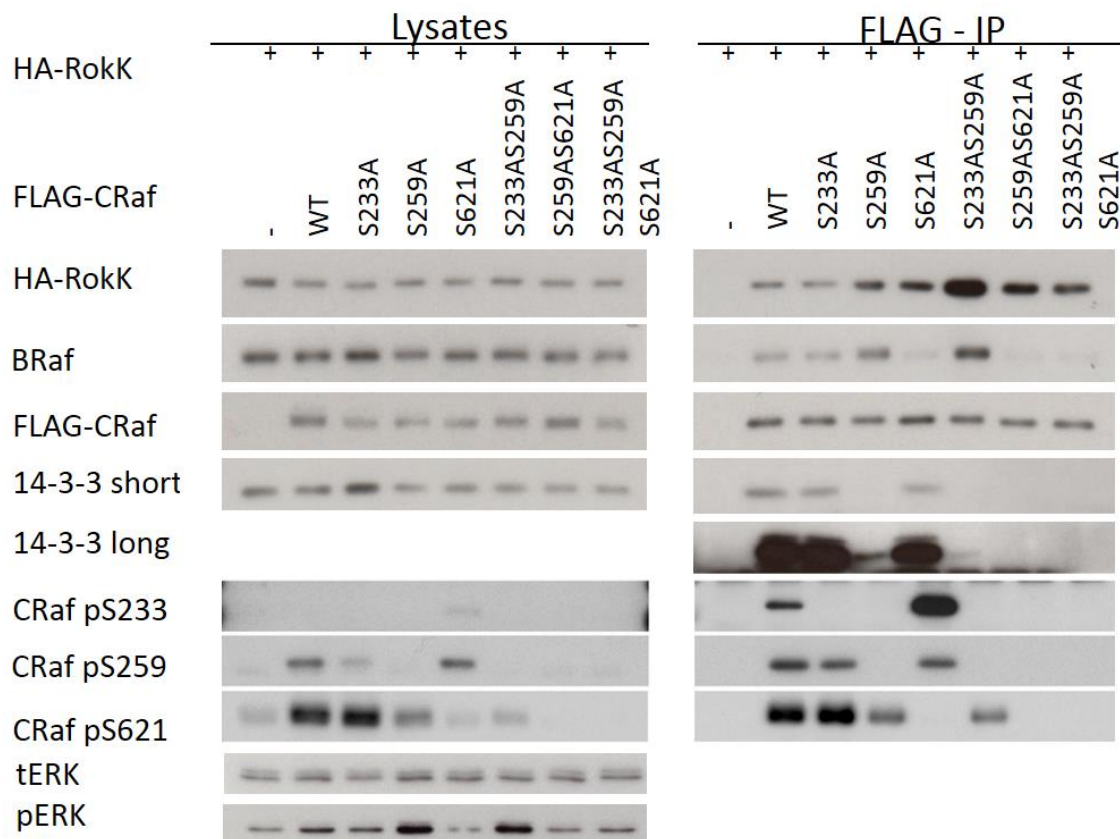
Figure 10 Immunoprecipitation experiment with 14-3-3 binding mutants of CRaf FLAG-tagged CRaf wild type and the single mutants S233A, S259A, S621A and two double mutants S233A/S259A, S259A/S621A as well as the triple mutant S233A/S259A/S621A were co-transfected together with HA-Rok-α kinase domain in Cos7 cells. CRaf was immunoprecipitated from the cells using FLAG-antibody. The co-precipitated HA-Rok kinase and endogenous BRaf were visualized by HA and BRaf antibodies. CRaf phosphosite specific antibodies were used to identify the phosphorylation state of the different CRaf constructs. CRaf pS233 specific antibody was too weak to give a signal in the whole cell lysate, only CRaf S621A transfected cells gave a weak signal.

Analysis of pERK levels allow the evaluation of activation of the ERK1/2 pathway by different CRaf constructs. The CRaf WT construct and to a greater extend the CRaf S259A and S233AS259A mutants increased ERK phosphorylation, while the S621A mutant behaved as a dominant negative regulator decreasing pERK levels independently of the presence of the other mutations introduced (i.e. single, double or triple mutants).

Consistently, the S259A and the S233AS259A mutation increased CRaf heterodimerization with BRaf, while the S621A mutation decreased it.

The interaction of CRAF with the Rok-α kinase domain was similarly regulated: The S259A and the S233AS259A mutations led to an increased interaction. However, while

phosphorylation of S621 was necessary for BRaf-CRaf interaction, the S621A mutant showed increased interaction with Rok-α compared to wild-type CRaf.

CRaf phosphosite-specific antibodies (S233/S259/S621) were used to confirm that these sites were not phosphorylated in the point mutants, and to also determine the general phosphorylation state of CRaf in immunoprecipitates. Interestingly, the antibody targeting pS233 did not show any signal when S259 was mutated. An explanation could be that S259 phosphorylation represents a prerequisite for binding of the antibody to pS233. The S621A mutant gave a strong signal in pS233 immunoblot, indicating that it was hyperphosphorylated on S233.

3.2.1 CRaf regulation by 14-3-3 and the impact on full length Rok-α

Next, I confirmed the results obtained using CRaf phosphosite mutants and the Rok-α kinase domain (**Figure 10**) and extended them to the interaction of CRaf with full-length Rok-α (see **Figure 11**). This test was critical since previous experiments had pointed out that the kinase domain of Rok-α is a stronger binding partner of CRaf compared to full-length Rok-α (Niault et al. 2009). Here I demonstrate a similar binding pattern of full length Rok-α (**Figure 11**) compared to binding of Rok-α kinase domain to the CRaf mutants (**Figure 10**), with one exception, the S259A CRaf mutant, which bound even stronger to full-length Rok-α than to the Rok-α kinase domain.

As shown in **Figure 11,** these results demonstrate that CRaf S259 de-phosphorylation plays a major role in positively regulating CRaf activity and dimer formation not only with BRaf, but also with Rok-α.
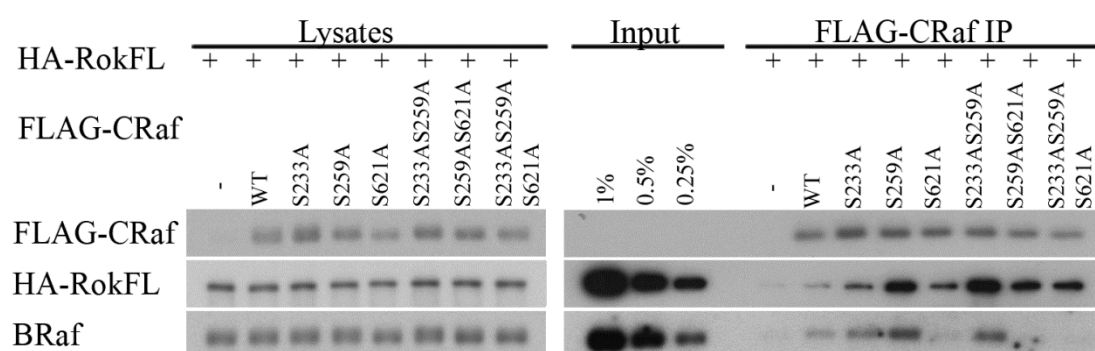
Figure 11 Immunoprecipitation experiment with co-transfected 14-3-3 binding mutants of CRaf and full length Rok-α FLAG-tagged CRaf wild type and the single mutants S233A, S259A, S621A and two double mutants S233A/S259A, S259A/S621A as well as the triple mutant S233A/S259A/S621A were transfected in this experiment. The FLAG-tagged CRaf

constructs were co-transfected with HA-Rok-α full length in Cos7 cells. FLAG Immunoprecipitation was done. Three different concentrations of cell lysate were loaded next to the immunoprecipitation to compare the amount of the co-immunoprecipitated Rok-α and BRaf.

3.3 Visualization of CRaf-Rok-α complexes in Cos7 cells: immunofluorescence studies

3.3.1 Visualization of CRaf and Rok-α by immunofluorescence

After investigating the interaction of CRaf-14-3-3 mutants with Rok-α by immunoprecipitation, I analyzed complex formation *in situ* by immunofluorescence and compared the CRaf S233A/S259A double mutant with the CRaf wild type. Both FLAG-tagged proteins were strongly expressed in the transfected Cos7 cells (**Figure 10**, **Figure 11**) and were distributed throughout the cytoplasm. The HA-Rok-α kinase domain was also strongly expressed in the transfected Cos7 cells and was not altered by the expression of WT or mutant CRaf. Nuclei were visualized with DAPI (4',6-diamidino-2-phenylindole) and filamentous actin was labeled with phalloidin, allowing the visualization of cell morphology. The FLAG-specific antibody showed some unspecific perinuclear staining. The HA antibody showed higher specificity for the HA-tag on Rok-α.
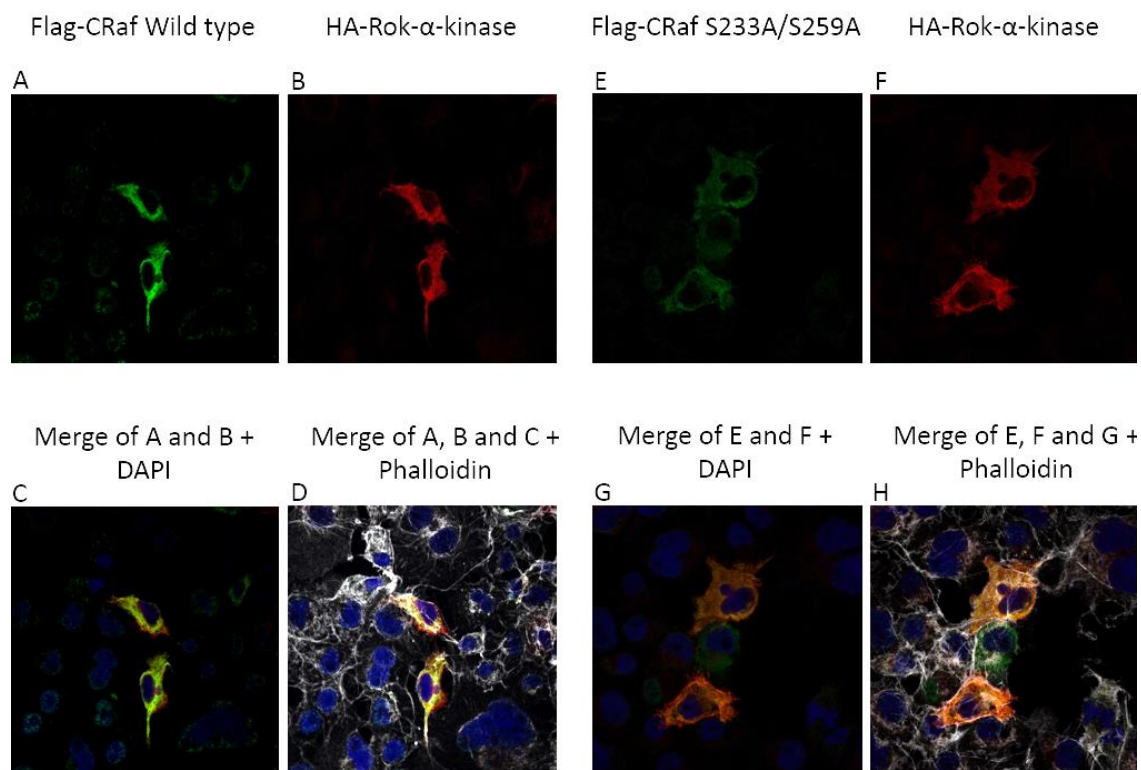

Figure 12 Immunofluorescence staining of co-transfected FLAG-tagged CRaf and HA-tagged Rok-α in Cos7 cells Co-transfected FLAG-CRaf wild type together with HA-Rok-α

kinase domain and FLAG-CRaf S233A/S259A mutant together with HA-Rok-α kinase domain in Cos7 cells. FLAG-CRaf wild type and FLAG-CRaf S233A/S259A mutant is visible in green, HA-Rok-α kinase domain is visible in red, DAPI is visible in blue and Phalloidin in white.

We could not observe any enrichment of CRaf or Rok-α at specific subcellular locations. In the merged image, co-localization of Rok-α (red) and CRaf (green) is shown in orange. However, these results do not demonstrate physical interaction.

3.3.2 Proximity ligation assay

Representative pictures of a proximity ligation assay (in-cell western) between different CRaf constructs and full length Rok-α are shown in **Figure 13**. The PLA followed the FLAG-immunoprecipitation western blot in terms of intensity of interaction (**Figure 11**). When wild type CRaf and full length Rok-α were overexpressed the signal increased compared to the empty vector transfected condition. As assessed by western blot (**Figure 11**) the S259A and also the S621A mutant increased the interaction with Rok-α compared to CRaf wild type. Again, CRaf double mutant S233AS259A was capable of further increasing the interaction. Mutation of the S233A residue alone did not influence CRaf/ Rok-α interaction; however, as observed in the immunoblot in Figure 11, S233AS259A double mutant strongly increased the proximity signal. Puzzlingly, the triple mutant (S233A/S259A/S621A) hardly increased the intensity of CRaf-Rok-α signal above wild type. This observation is not consistent with the results obtained in the western blot (**Figure 11**), showing that the triple mutant co-immunoprecipitated more Rok-α than the wild type CRaf construct. It is possible that PLA is not sensitive enough to visualize this difference. As shown by immuno-fluorescence experiments (**Figure 13**) the distribution of the interacting partners was unchanged. Together these results show that mutation of CRaf affects the interaction with Rok-α but not the distribution of the CRaf-Rok-α complex in Cos7 cells.
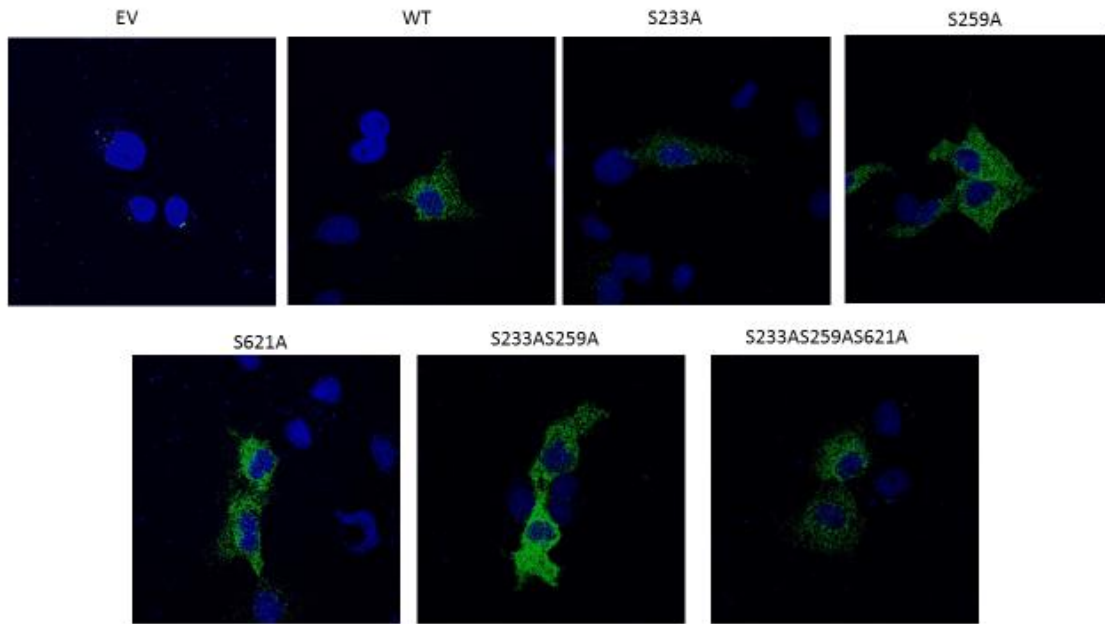
Figure 13 Proximity ligation assay of FLAG-tagged CRaf constructs and HA-tagged Rok-α FLAG-tagged wild type CRaf and the single mutants S233A, S259A, S621A and two double mutants S233A/S259A, S259A/S621A as well as the triple mutant S233A/S259A/S621A were transfected in this experiment (EV: empty vector, WT: wild type). These FLAG-tagged CRaf constructs were co-transfected with full length HA-Rok-α in Cos7 cells. Proximity ligation assay was performed with antibodies against CRaf and Rok-α. The PLA probe is shown in green and DAPI nuclear staining in blue. **Figure 11** shows the lysates of the plates where the coverslips for the proximity ligation assay were added.

3.4 Do BRaf and Rok-α compete for CRaf binding?

In the next experiments I investigated the dependency of CRaf and BRaf or Rok-α complex formation by increasing the amount of the individual interacting partners of CRaf. Furthermore, I tested the effect of this manipulation on CRaf's interaction with the respective other partner.

3.4.1 Rok-α/BRaf overexpression

If BRaf and Rok-α compete for CRaf, one would expect an increase in BRaf and a simultaneous decrease in Rok-α in CRaf immunoprecipitates prepared from cells over-expressing BRaf. Conversely, Rok-α overexpression should result in an increase in CRaf/Rok-α complexes at the expenses of CRaf/BRaf complexes. To further investigate this hypothesis, I overexpressed Rok-α in Cos7 cells and immunoprecipitated CRaf. If BRaf and Rok-α would compete for CRaf, increased amount of Rok-α should decrease the amount of co-immunoprecipitated BRaf.
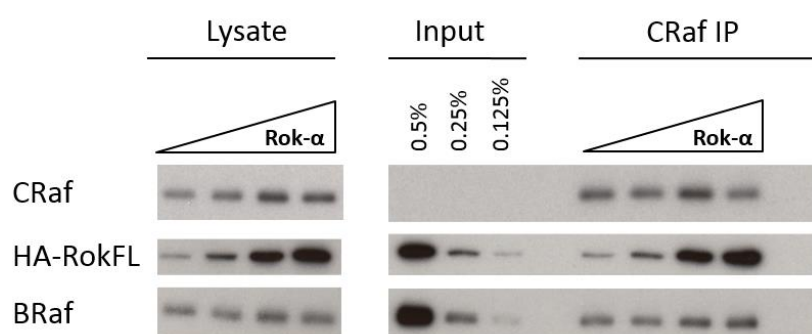
Figure 14 Rok-α over-expression followed by CRaf immunoprecipitation in Cos7 cells
Stepwise increase of Rok-α overexpression (0/0.5/2/4 μg plasmid) followed by CRaf-immuno-precipitation. Three different concentrations of cell lysate were loaded next to the immunopre-cipitation to directly compare the amount of the co-immunoprecipitated Rok-α and BRaf.

Increasing concentrations of Rok-α are visible in the input lane (**Figure 14**). CRaf was able to co-immunoprecipitate increased amounts of Rok-α. BRaf co-immunoprecipitation, however, did not show any changes when Rok-α binding increased; thus, increased CRaf/Rok-α interaction did not affect the CRaf – BRaf dimerization.

To study whether BRaf has the ability to pull Rok-α away from CRaf and in order to generally investigate protein complex formation during BRaf overexpression, I transfected BRaf in Cos7 cells and performed CRaf immunoprecipitation (**Figure 15**).
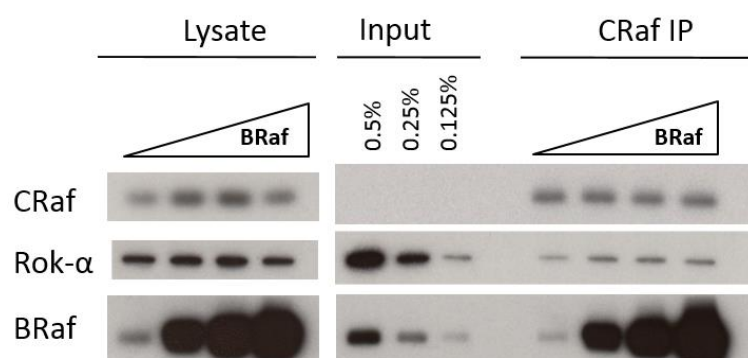
Figure 15 Stepwise increase of BRaf overexpression (0/0.5/2/4 µg plasmid) in Cos7 cells, followed by CRaf-immunoprecipitation

The stepwise overexpression of BRaf is visible in the input lane. CRaf efficiently co-immunoprecipitated increased amounts of BRaf. This increase of co-immunoprecipitated BRaf did not reduce Rok-α co-immunoprecipitation.

Based on the results obtained in these two experiments (**Figure 14**, **Figure 15**) we conclude that Rok-α and BRaf are not competing for CRaf binding in Cos7 cells.

3.4.2 CRaf wild type/S621A comparison

The results discussed above are consistent with the hypothesis that BRaf and Rok-α bind to different species of CRaf. This implies a further level of complexity. The experiments utilizing phosphosite mutants (**Figure 10 and Figure 11**) demonstrated that the phosphorylation of S621 can potentially provide such regulation. To test this hypothesis, I overexpressed WT CRaf and its S621A mutant and tested the interaction of these two proteins with endogenous Rok-α and BRaf. Three different concentrations of wild type CRaf and the S621A mutant were transfected into Cos7 cells. FLAG and Rok-α immunoprecipitation were performed from the same cell lysates.
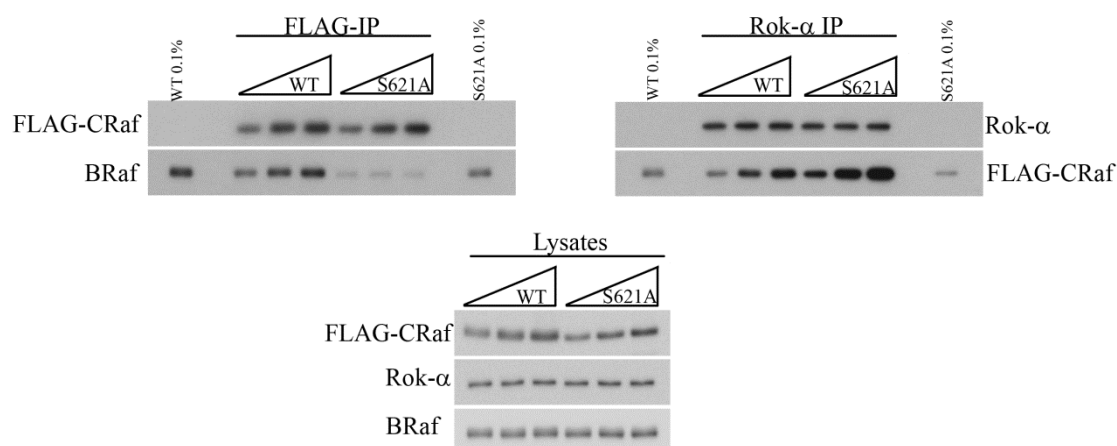
Figure 16 Stepwise overexpression of wild type FLAG-CRaf and FLAG-CRaf S621A mutant in Cos7 cells Two immunoprecipitations were done using the same lysate; FLAG and Rok-α immunoprecipitation. 0.1% of the lysate used for the immuno-precipitation was loaded next to the immunoprecipitation. The first sample of the input (wild type CRaf) were loaded in the first slot and the fourth sample (S621A mutant) in the last slot.

Stepwise overexpression of the FLAG-tagged CRaf wild type and CRaf S621A mutant is visible in the input lane (**Figure 16**). Increased amounts of CRaf in cell lysates were also reflected in the FLAG immunoprecipitation. The FLAG immunoprecipitation confirmed the decreased affinity of BRaf for the CRaf S621A mutant compared to wild type CRaf. More BRaf was co-immunoprecipitated by the increasing amounts of wild type, but not S621A CRaf.

Endogenous Rok-α was barely detectable in the FLAG immunoprecipitates; however, Rok-α co-immunoprecipitation showed that both CRaf WT and the S621A mutants co-immunoprecipitated in amounts proportional to the expression of the constructs, and indeed, in cases of similar construct expression, CRaf S621A co-immunoprecipitated more efficiently than WT CRaf.

These results are consistent with the hypothesis that S621 phosphorylation discriminates between BRaf and Rok-α binding.

4 Discussion

RAF is the signaling link between Ras and Mek in the ERK1/2-pathway (reviewed in Lavoie & Therrien 2015). CRaf can interact with different kinases and other signal transducers that are not involved in the ERK1/2-pathway. 4 main partners that contribute to cell motility, survival and differentiation have been described: BRaf, MST2, ASK1, and Rok-α (reviewed in Varga & Baccarini 2012).

The interaction of CRaf and Rok-α, which is necessary for the maintenance of Ras-induced epidermal tumors in mice (Ehrenreiter et al. 2009), was the focus of my studies. The short term goal of my experiments was to obtain insights into the molecular details of the interaction between CRaf and Rok-α. The long term goal of this study is the design of specific inhibitors to disrupt this interaction, which might pave the way for the (co-)treatment of tumors driven by Ras.

The first question addressed here focused on the localization of the Rok-α specific binding site on CRaf. The C-terminal truncation experiment (**Figure A1**), suggests that the large lobe of the CRaf kinase domain is not necessary for complex formation with Rok-α. The experiment also implies that the main binding region of Rok-α is localized on the N-lobe of CRaf's kinase domain. Alternatively, the presence of CRaf`s kinase domain (with or without the large C-lobe) may change the conformation of the N-terminal part, increasing its affinity for Rok-α. Finally, we can conclude that the N-terminal regulatory domain of CRaf has a preference to bind to Rok-α, but not to BRaf. Thus, CRaf might discriminate between the two interactors via its N-terminal regulatory domain.

BRaf needs an intact CRaf kinase domain for interaction (Eisenhardt et al. 2016) and it dimerizes with CRaf in a side-to-side manner, similarly to the homodimer structures of both BRaf and CRaf obtained by X-ray crystallography (reviewed in Lavoie et al. 2015). C-terminal truncated CRaf failed to bind BRaf (**Figure A1**). This is in accordance with the literature showing that the phosphorylation of the critical residue S621 (localized on the C-lobe of the kinase domain) is necessary for correct folding of the kinase domain (Noble et al. 2008) and also for binding to BRaf (reviewed in Lavoie et al. 2015 and also see **Figure 10**).

CRaf lacking the Ras binding domain (construct 131-648 compared to 1-648) had a reduced affinity for Rok-α (**Figure 9**). It is well known that Ras binding induces a conformational change in CRaf (Hibino et al. 2009), which switches CRaf from a closed to an open conformation. A Ras-binding deficient mutant of CRaf (R89L) has an impaired binding to Rok-α (Niault et al. 2009), implying that Ras binding is a prerequisite for interaction with Rok-α. In addition, co-transfection with a constitutively active Ras mutant also increased this interaction. Ras binding also increases the interaction of CRaf with BRaf (reviewed in Lavoie et al. 2015), which was confirmed by my experiments.

The experiments in **Figure 9**, **Figure 10**, **Figure A1**, **Figure A2** shed light onto the CRaf–Rok-α interaction, indicating the importance of CRaf kinase domain to form a stable complex with both Rok-α and BRaf.

Previous data showed that the CRaf regulatory domain interacts with the Rok-α kinase domain (Niault et al. 2009). In my experiment (**Figure A1**) the regulatory domain of CRaf immunoprecipitates Rok-α kinase domain. Interestingly all CRaf truncations used here were able to co-immunoprecipitate Rok-α. The N-lobe of CRaf kinase domain seemed to play a major role in CRaf-Rok-α interaction because its presence significantly increased Rok-α kinase domain co-immunoprecipitation. Unfortunately, I could not investigate if those CRaf constructs impact on Rok-α kinase activity. This has previously been shown for the CRaf regulatory domain (Niault et al. 2009).

Further studies e.g. solving the crystal structure are needed to understand the interaction in molecular detail. However, by using cellular models we inform on the properties and requirements of *in vitro* produced CRaf species for interaction studies with recombinant proteins.

Since the conformational status of CRaf is also regulated through the binding of 14-3-3 proteins to distinct phosphorylation sites of CRaf, my aim was to analyze the impact of these regulatory phosphorylation sites in CRaf species on binding to Rok-α.

In addition to the well-known S259 and S621 14-3-3 binding sites on CRaf, S233 was recently investigated by Molzan and colleagues (Molzan & Ottmann 2012). This additional site raises the question how CRaf is regulated by 14-3-3 dimers having three possible binding sites on the CRaf molecule. The N-terminal (S259) 14-3-3 binding site phosphorylation counteracts Ras binding and hetero-dimerization with BRaf. Additionally, interaction with BRaf is decreased when the C-terminal 14-3-3 binding site (S621) is not phosphorylated (Garnett et al. 2005).

S621 phosphorylation on CRaf is essential for BRaf binding, since the S621A alone or in combination with the other 14-3-3 sites (S621A single mutant, S621A/S259A double mutant and S621A/S259A/S233A triple mutant), reduced BRaf binding to CRaf to an almost undetectable level. These results confirm published data showing that S621A mutants function as dominant negative regulators for BRaf binding and thus for ERK activation.

The CRaf S259A mutation and the S259A/S233A mutation increased the phospho-ERK levels even further compared to the CRaf wild type construct (**Figure 10**). This is in line with a previously published role of phosphorylated S259 counteracting Ras binding. PP2A dephosphorylation of S259 occurs in the cytosol (Kubicek et al. 2002) and is a prerequisite for Ras binding at the membrane and thus increased affinity for BRaf.

The co-immunoprecipitation of 14-3-3 adaptor protein with the CRaf constructs (**Figure 10**), suggests that these 3 positions are the main regulators on CRaf for 14-3-3 binding. There is no 14-3-3 detectable in the co-immunoprecipitation of the CRaf triple mutant (S233A/S259A/S621A). Interestingly, the C-terminal binding site bound less 14-3-3 compared to the N-terminal binding site. The question arises of whether both sites bind 14-3-3 dimers, as suggested by Molzan and colleagues (Molzan & Ottmann 2012).

I confirm the binding of 14-3-3 to CRaf wild type, S233A, S259A or S233A/S259A mutants by co-immunoprecipitation (**Figure 10**) that was also investigated by Molzan and colleagues (Molzan & Ottmann 2012), who studied 14-3-3 ζ binding to the phosphorylated peptides by isothermal titration calorimetry and fluorescence polarization. In this study, di-phosphorylated CRaf S259/S233 showed the strongest affinity for 14-3-3 ζ. The S259 mono-phosphorylated peptide showed lower affinity while the S233 mono-phosphorylated CRaf peptide showed the lowest (Molzan & Ottmann 2012).

S621A mutation removes the 14-3-3 protein from the C-terminal domain of CRaf (Light et al. 2002). This might lead to an unstable interaction of CRaf with BRaf, because the C-terminal 14-3-3 dimer is thought to stabilize the heterodimer of BRaf with CRaf (reviewed in Lavoie et al. 2015). At the same time, Rok-α had an increased affinity for CRaf in the absence of bound 14-3-3 at the C-terminal end of CRaf. This suggests that the C-terminal 14-3-3 disfavors Rok-α binding to CRaf. On the other hand, if S621 is not phosphorylated, this might change the conformation of the kinase domain of CRaf. Such new conformation might have a preference for Rok-α binding. Another possibility could be that Rok-α stabilizes CRaf and inhibits its degradation (Noble et al. 2008) when S621 is not phosphorylated.

BRaf - CRaf and CRaf - Rok-α interaction was increased when S259 alone or both S259 and S233 were dephosphorylated. The phosphorylation state of CRaf's N-terminal 14-3-3 binding site regulates CRaf – BRaf and CRaf – Rok-α interaction at the same time. Thus, CRaf might discriminate between activating the Erk1/2-pathway and inhibiting Rok-α signaling to LIM kinase changing its S621 phosphorylation status.

Previous studies revealed that both S233 and S259 have to be dephosphorylated for membrane recruitment and Ras binding (Molzan & Ottmann 2012). This data was obtained by immunofluorescence experiments. GFP-tagged CRAF330ΔC S259A mutant (containing only the N-terminal regulatory domain of CRaf), co-transfected with mCherry-HRas, co-localized at the plasma membrane in HEK293T cells. The GFP-CRAF330ΔC wild type was hardly recruited to the membrane by mCherry-HRas co-transfection, and was evenly distributed in the cytoplasm. GFP-CRAF330ΔC S233A mutant showed an intermediate behavior. It was not recruited to the membrane to the same extent as observed for the S259A mutant, but to a higher degree than the CRaf wild type construct (Molzan & Ottmann 2012). This represents an example of how one

phosphorylation event can critically alter the distribution of CRaf inside the cell. These experiments raised the idea of investigating the distribution of CRaf 14-3-3 mutants by co-transfecting Rok-α kinase domain in Cos7 cells, but I could not observe any redistribution of the CRaf-Rok- α complexes upon mutation. In mouse embryonic fibroblasts, CRaf regulatory domain and Rok-α co-localize on vimentin cytoskeleton (Niault et al. 2009). In order to test whether this is the case for the 14-3-3 binding site mutants, immunofluorescence experiments were performed. If localization plays a role in regulating CRaf – Rok-α interaction I would have expected to see a difference between CRaf wild type and the CRaf S233A/S259A double mutant in an immunofluorescence experiment. The increase in interaction, which was visible following FLAG-immunoprecipitation of CRaf S233A/S259A with HA-tagged-Rok-α kinase domain (**Figure 10**), was noteworthy. Although Rok-α co-localized with CRaf in the immunofluorescence experiment, no change in distribution was observed for CRaf S233A/S259A mutant (**Figure 12**). Furthermore, no morphological change or other visible effect was found when comparing the CRaf wild-type with the CRaf S233A/S259A mutant transfected cells (**Figure 12**). The proximity ligation assay (**Figure 13**) also failed to give any hint about CRaf's phosphorylation state, that would have been indicated by an enrichment, for CRaf-Rok-α interaction, at a specific compartment in Cos7 cells (? Correct or did I misunderstand). These results highlight that additional studies are needed to highlight further details and to better understand the regulation of CRaf-Rok-α interaction.

The analysis of CRaf 14-3-3 mutants (**Figure 10-13)** clearly demonstrated that both BRaf and Rok-α do bind stronger to dephosphorylated CRaf S233/S259 than to wild type CRaf. Experiments using truncated CRaf (**Figure 9, Figure A1** and **Figure A2**) showed that BRaf and Rok-α partially share the same binding domain on CRaf. Therefore, I hypothesized that BRaf and Rok-α might compete for CRaf binding.

To investigate this aspect, one of the interacting partners of CRaf (Rok-α or BRaf) was overexpressed (**Figure 14** and **Figure 15**). CRaf was able to co-immunoprecipitate increased amounts of Rok-α (**Figure 14**). This result suggest that CRaf is not saturated with Rok-α in steady state growing Cos7 cells. Therefore, more Rok-α can be bound. At the same time, the increased concentration of Rok-α in Cos7 cells did not affect CRaf – BRaf heterodimerization. This result implies that Rok-α does not disrupt CRaf – BRaf interaction. The same conclusion can be drawn from BRaf overexpression experiments (**Figure 15**). BRaf overexpression did not alter the amount of co-immunoprecipitated Rok-α. In addition, endogenous CRaf was able to bind more BRaf without reducing CRaf - Rok-α interaction. Based on the results obtained by these two experiments (**Figure 14**, **Figure 15**) one can conclude that Rok-α and BRaf are not competing for CRaf binding in Cos7 cells.

The result of **Figure 14** and **Figure 15** imply that another mechanism has to be behind CRaf discriminating between Rok-α or BRaf binding. So I came back to the hypothesis of BRaf and Rok-α binding to different species of CRaf.

To test this hypothesis CRaf was overexpressed at different concentrations (**Figure 16**). Both BRaf and Rok-α bound increasing amount of CRaf with increasing their own concentration. The S621A mutant, used as a control, showed that BRaf cannot efficiently bind to it, while instead Rok-α is able to bind more CRaf S621A if the concentration of this mutant is increased. The Rok-α immunoprecipitation (**Figure 16**) confirmed that Rok-α binds more efficiently to CRaf S621A mutant than to wild type CRaf. This increased interaction of CRaf S621A with Rok-α could be due to a stabilizing effect of CRaf S621A mutant by Rok-α. To investigate whether this was due to preventing degradation by the proteasome, proteasome inhibition and Rok silencing was performed in CRaf wild type and CRaf S621A transfected Cos7 cells (**Figure A3**). Noble et al. 2008 previously showed that CRaf S621A is degraded by the proteasome. My experiment instead did not show that silencing of Rok-α increased CRaf S621A degradation (**Figure A3**). Probably the observed phenotype is caused through a distinct mechanism, rather than protection of CRaf S621A mutant by Rok-α from proteasomal degradation.

In spite of the fact that CRaf has to be activated for complex formation with both BRaf and Rok-α (dephosphorylation of S259 and also S233 possibly) and that the binding sites overlap at least partially on the kinase domain of CRaf, the two binding partners do not compete with each other for CRaf binding.

This phenomenon indicates that inside the cells, BRaf and Rok-α bind to differentially phosphorylated species: BRaf requires S621 phosphorylation on CRaf, while Rok-α does not. Another possible explanation is that BRaf and Rok-α differential localize inside the cell, while they can still bind the same CRaf species. However, the second theory is not supported by the results obtained in the course of the proximity ligation assay.

5   References

Bravo-Cordero, J.J. et al., 2013. Functions of cofilin in cell locomotion and invasion. *Nature reviews. Molecular cell biology*, 14(7), p.10.1038/nrm3609. Available at: http://www.ncbi.nlm.nih.gov/pmc/articles/PMC3878614/.

Chong, H., Lee, J. & Guan, K.L., 2001. Positive and negative regulation of Raf kinase activity and function by phosphorylation. *The EMBO journal*, 20(14), pp.3716–3727.

Davies, H. et al., 2002. Mutations of the BRAF gene in human cancer. *Nature*, 417(6892), pp.949–954. Available at: http://www.ncbi.nlm.nih.gov/pubmed/12068308.

Dhillon, A.S. et al., 2007. Phosphatase and feedback regulation of Raf-1 signaling. *Cell Cycle*, 6(1), pp.3–7. Available at: http://www.ncbi.nlm.nih.gov/pubmed/17218791.

Dominguez-Sola, D. et al., 2007. Non-transcriptional control of DNA replication by c-Myc. *Nature*, 448(7152), pp.445–451. Available at: http://dx.doi.org/10.1038/nature05953.

Ehrenreiter, K. et al., 2009. Raf-1 addiction in Ras-induced skin carcinogenesis. *Cancer Cell*, 16(2), pp.149–160. Available at: http://www.ncbi.nlm.nih.gov/pubmed/19647225.

Ehrenreiter, K. et al., 2005. Raf-1 regulates Rho signaling and cell migration. *J Cell Biol*, 168(6), pp.955–964. Available at: http://www.ncbi.nlm.nih.gov/pubmed/15753127.

Eisenhardt, A.E. et al., 2016. Phospho-proteomic analyses of B-Raf protein complexes reveal new regulatory principles. *Oncotarget*, 7(18), pp.26628–26652.

Emerson, S.D. et al., 1995. Solution structure of the Ras-binding domain of c-Raf-1 and identification of its Ras interaction surface. *Biochemistry*, 34(21), pp.6911–6918.

Garnett, M.J. et al., 2005. Wild-type and mutant B-RAF activate C-RAF through distinct mechanisms involving heterodimerization. *Mol Cell*, 20(6), pp.963–969. Available at: http://www.ncbi.nlm.nih.gov/pubmed/16364920.

GmbH, 5 Prime, 2009. PerfectPrep ™ EndoFree Maxi Kit Manual. Available at: http://www.5prime.com/media/29658/manual perfectprep endofree maxi_1048300_jan2009.pdf.

Hanahan, D. & Weinberg, R.A., 2011. Hallmarks of cancer: the next generation. *Cell*, 144(5), pp.646–674.

Hatzivassiliou, G. et al., 2010. RAF inhibitors prime wild-type RAF to activate the MAPK pathway and enhance growth. *Nature*, 464(7287), pp.431–435. Available at: http://www.ncbi.nlm.nih.gov/pubmed/20130576.

Hibino, K. et al., 2009. A RasGTP-induced conformational change in C-RAF is essential for accurate molecular recognition. *Biophysical journal*, 97(5), pp.1277–87. Available at: http://www.sciencedirect.com/science/article/pii/S0006349509010595 [Accessed September 25, 2015].

Hu, J. et al., 2013. Allosteric activation of functionally asymmetric RAF kinase dimers. *Cell*, 154(5), pp.1036–1046. Available at: http://www.ncbi.nlm.nih.gov/pubmed/23993095.

Julian, L. & Olson, M.F., 2014. Rho-associated coiled-coil containing kinases (ROCK): structure, regulation, and functions. *Small GTPases*, 5(2), p.e29846.

Kubicek, M. et al., 2002. Dephosphorylation of Ser-259 regulates Raf-1 membrane association. *The Journal of biological chemistry*, 277(10), pp.7913–7919.

Lavoie, H. & Therrien, M., 2015. Regulation of RAF protein kinases in ERK signalling. *Nature reviews. Molecular cell biology*, 16(5), pp.281–298.

Light, Y., Paterson, H. & Marais, R., 2002. 14-3-3 Antagonizes Ras-Mediated Raf-1 Recruitment to the Plasma Membrane To Maintain Signaling Fidelity. *Molecular and Cellular Biology*, 22(14), pp.4984–4996. Available at: http://www.ncbi.nlm.nih.gov/pmc/articles/PMC139778/.

Marenholz, I. et al., 2001. Identification of human epidermal differentiation complex (EDC)-encoded genes by subtractive hybridization of entire YACs to a gridded Keratinocyte cDNA library. *Genome Research*, 11(3), pp.341–355.

Mebratu, Y. & Tesfaigzi, Y., 2009. How ERK1/2 activation controls cell proliferation and cell death: Is subcellular localization the answer? *Cell Cycle*, 8(8), pp.1168–1175.

Miyazaki, K., Komatsu, S. & Ikebe, M., 2006. Dynamics of RhoA and ROKalpha translocation in single living cells. *Cell biochemistry and biophysics*, 45(3), pp.243–254.

Molzan, M. & Ottmann, C., 2012. Synergistic binding of the phosphorylated S233-and S259-binding sites of C-RAF to one 14-3-3Î¶ dimer. *Journal of molecular biology*, 423(4), pp.486–495.

Mott, H.R. et al., 1996. The solution structure of the Raf-1 cysteine-rich domain: a novel ras and phospholipid binding site. *Proc Natl Acad Sci U S A*, 93(16), pp.8312–8317.

Nakamura, Y. et al., 2006. Marked increase of insulin gene transcription by suppression of the Rho/Rho-kinase pathway. *Biochemical and biophysical research communications*, 350(1), pp.68–73. Available at: http://www.sciencedirect.com/science/article/pii/S0006291X06020110 [Accessed September 21, 2015].

Newlaczyl, A.U. et al., 2014. Decoding RAS isoform and codon-specific signalling. *Biochemical Society transactions*, 42(4), pp.742–746.

Niault, T. et al., 2009. From autoinhibition to inhibition in trans: the Raf-1 regulatory domain inhibits Rok-alpha kinase activity. *J Cell Biol*, 187(3), pp.335–342. Available at: http://www.ncbi.nlm.nih.gov/pubmed/19948477.

Niihori, T. et al., 2006. Germline KRAS and BRAF mutations in cardio-facio-cutaneous syndrome. *Nat Genet*, 38(3), pp.294–296.

Noble, C. et al., 2008. CRAF autophosphorylation of serine 621 is required to prevent its proteasome-mediated degradation. *Mol Cell*, 31(6), pp.862–872. Available at: http://www.ncbi.nlm.nih.gov/pubmed/18922468 [Accessed June 15, 2015].

Ohashi, K. et al., 2000. Rho-associated kinase ROCK activates LIM-kinase 1 by phosphorylation at threonine 508 within the activation loop. *J Biol Chem*, 275(5), pp.3577–3582.
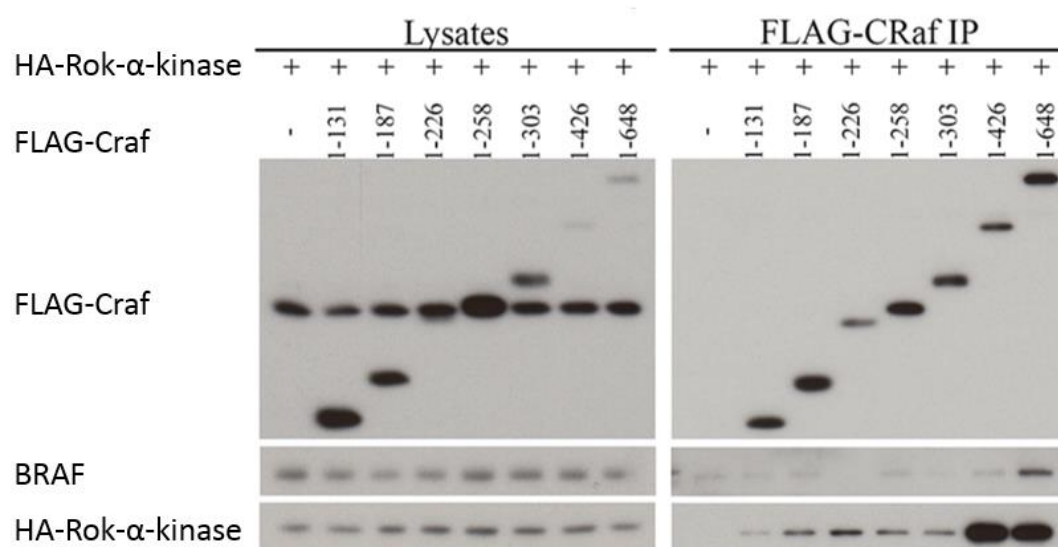
Pandit, B. et al., 2007. Gain-of-function RAF1 mutations cause Noonan and LEOPARD syndromes with hypertrophic cardiomyopathy. *Nat Genet*, 39(8), pp.1007–1012.

Prestained, P. & Ladder, P., 2009. PageRuler ™ Prestained Protein Ladder (10 – 170 kDa). , p.2009.

Rauen, K.A., 2013. The RASopathies. *Annu Rev Genomics Hum Genet*, 14, pp.355–369.

Razzaque, M.A. et al., 2007. Germline gain-of-function mutations in RAF1 cause Noonan syndrome. *Nat Genet*, 39(8), pp.1013–1017.

Riento, K. & Ridley, A.J., 2003. Rocks: multifunctional kinases in cell behaviour. *Nat Rev Mol Cell Biol*, 4(6), pp.446–456.

Rodriguez-Viciana, P. et al., 2006. Germline mutations in genes within the MAPK pathway cause cardio-facio-cutaneous syndrome. *Science*, 311(5765), pp.1287–1290.

Salzano, M. et al., 2012. Calcium/calmodulin-dependent protein kinase II (CaMKII) phosphorylates Raf-1 at serine 338 and mediates Ras-stimulated Raf-1 activation. *Cell Cycle*, 11(11), pp.2100–2106.

Santarpia, L., Lippman, S.M. & El-Naggar, A.K., 2012. Targeting the MAPK-RAS-RAF signaling pathway in cancer therapy. *Expert Opin Ther Targets*, 16(1), pp.103–119. Available at: http://www.ncbi.nlm.nih.gov/pubmed/22239440.

Shimizu, K. et al., 1994. Synergistic activation by Ras and 14-3-3 protein of a mitogen-activated protein kinase kinase kinase named Ras-dependent extracellular signal-regulated kinase kinase stimulator. *The Journal of biological chemistry*, 269(37), pp.22917–22920.

Trifilieff, P. et al., 2013. Complexes in the Striatum. *Brain*, 51(2), pp.111–118.

Varga, A. & Baccarini, M., 2012. RAF-1 (C-RAF). *Encyclopedia of Signaling Molecules*, pp.1562–1570.

Wimmer, R. et al., 2012. Angiogenic sprouting requires the fine tuning of endothelial cell cohesion by the Raf-1/Rok-alpha complex. *Dev Cell*, 22(1), pp.158–171. Available at: http://www.ncbi.nlm.nih.gov/pubmed/22209329.
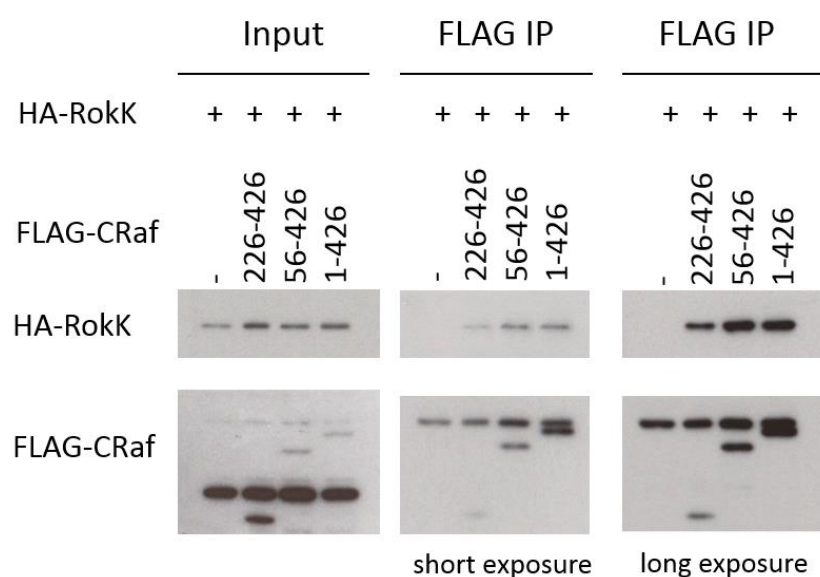
Webpages:

(http://www.who.int/cancer/en/)

6   Appendix

6.1   C-terminal-truncation

Figure A1 Transfection of Cos7 cells with different FLAG-tagged CRaf constructs which differ in length Those cells were co-transfected with HA-tagged Rok-α kinase domain. FLAG immunoprecipitation was done.

6.2   N-terminal Ras binding domain truncations

Figure A2 The impact of removing CRaf´s Ras binding domain on Rok-α binding Transfection of Cos7 cells with different FLAG-tagged CRaf constructs that differ in length. Those cells were co-transfected with HA-tagged Rok-α kinase domain. FLAG immunoprecipitation was performed. The CRaf Ras binding domain starts at residue 55 and ends at residue 131.

6.3 Proteasome inhibition
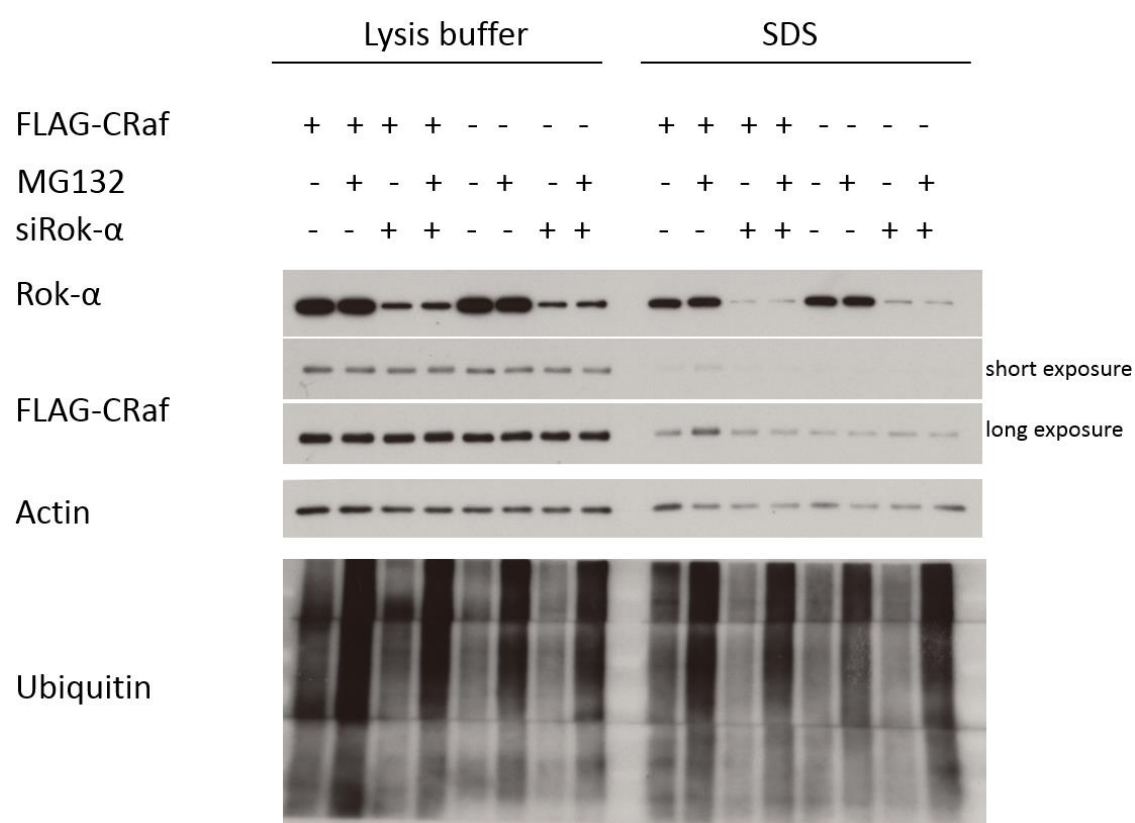
Figure A3 Proteasome inhibition and Rok silencing in CRaf wild type and CRaf S621A transfected Cos7 cells CRAF: Wt: +, S621A: -, MG132: DMSO: -, MG132: +, Day 1: siRok-α. Day 2: CRaf wt/S621A transfection. Day 3: MG132 treatment. Day 4: Harvest the cells.